

# Sediment sorting at the Sand Motor at storm and annual time scales



B.J.A. Huisman<sup>a, b, \*</sup>, M.A. de Schipper<sup>a, c</sup>, B.G. Ruessink<sup>d</sup>

<sup>a</sup>Delft University of Technology, Faculty of Civil Engineering and Geosciences, Department of Hydraulic Engineering, P.O. Box 5048, 2600GA Delft, The Netherlands

<sup>b</sup>Deltares, Unit Hydraulic Engineering, Department of Harbour, Coastal and Offshore Engineering, P.O. Box 177, 2600MH Delft, The Netherlands

<sup>c</sup>Shore Monitoring and Research, P.O. Box 84070, 2508AB The Hague, The Netherlands

<sup>d</sup>Utrecht University, Faculty of Geosciences, Department of Physical Geography, P.O. Box 80115, Utrecht 3508TC, The Netherlands

## ARTICLE INFO

### Article history:

Received 25 April 2016

Received in revised form 29 July 2016

Accepted 6 September 2016

Available online 12 September 2016

### Keywords:

Nourishment

Bed sediment

Alongshore heterogeneity

Sorting

Morphology

## ABSTRACT

Bed sediment composition, with a focus on the median grain size  $D_{50}$ , was investigated at a large-scale nourishment (The ‘Sand Motor’) at the Dutch coast (~21.5 million m<sup>3</sup> sand). Considerable alongshore heterogeneity of the bed composition ( $D_{50}$ ) was observed as the Sand Motor evolved over time with (1) coarsening of the exposed part of the Sand Motor (+90 to +150  $\mu$ m) and (2) a depositional area with relatively fine material (50  $\mu$ m finer) just North and South of the Sand Motor. The alongshore heterogeneity of the measured  $D_{50}$  values was most evident outside the surfzone (i.e. seaward of MSL –4 m). Coarsening of the bed after construction of the Sand Motor was attributed to hydrodynamic sorting processes, because the alongshore heterogeneity of the  $D_{50}$  showed a similar spatial pattern as the mean bed shear stresses. The observed alongshore heterogeneity of the  $D_{50}$  and correlation of  $D_{50}$  with modelled mean bed shear stresses suggest that preferential erosion of the finer sand fractions has taken place. The selective transport of finer sand fractions results in a coarser top layer of the bed at the Sand Motor. The preferential transport is most dominant during mild and moderate conditions when hydrodynamic forcing conditions are close to the critical bed shear stresses for transport. The measurements also show the impact of a storm, which consists of a ~40  $\mu$ m finer  $D_{50}$  of the offshore bed composition in front of the Sand Motor (i.e. where a considerably coarser bed was in place). Additionally, storms may generate a (temporary) zone with fine bed material at the toe of the deposition profile. This means that the coarsening of the bed is reduced by storms as a result of the mobilization of both coarse and fine sediment and mixing of the bed with the relatively finer substrate.

© 2016 Published by Elsevier B.V.

## 1. Introduction

Spatial heterogeneity of bed sediment composition is observed at many coasts around the world (Holland and Elmore, 2008), but seldom accounted for in morphological or environmental impact studies of coastal interventions (e.g. modelling of sand nourishments; Capobianco et al., 2002). Knowledge of the potential spatial variability of the bed sediment (i.e. grain size and grading) is however considered essential for the understanding of the ecological impact of large-scale coastal interventions. Firstly, bed composition changes affect the ecological habitats for benthic species and fish (e.g. McLachlan, 1996; Knaapen et al., 2003). Small changes in the top-layer (i.e. centimeters) grain size can, for example, significantly affect the burrowing ability of juvenile plaice (Gibson and Robb, 1992). Secondly, long-term morphological changes may be

affected by bed coarsening when finer sand fractions are predominantly eroded (Van Rijn, 2007). Furthermore, the development of the morphology of rip-bar systems was found to be inter-related with the bed sediment (Gallagher et al., 2011; Dong et al., 2015).

Spatial heterogeneity of the bed composition of natural coasts is characterized by a fining of sediment grain size in the offshore direction with coarsest sediment being found in the swash zone (Inman, 1953; Sonu, 1972; Liu and Zarillo, 1987; Horn, 1993; Pruszk, 1993; Stauble and Cialone, 1996; Kana et al., 2011). In the presence of sub-tidal bars the spatial pattern of the bed sediment composition can vary between different studies. Generally, coarser sediment is observed in the bar troughs and finer sediment on bar crests (Moutzouris et al., 1991; Katoh and Yanagishima, 1995), but Van Straaten (1965) observed coarser material on the bar crests for the Dutch coast. Considerable spatial heterogeneity of the sediment grain size was also observed at rip-bar systems with coarser surface sediment in the rip-channel and finer sediment at the head of the transverse bar (MacMahan et al., 2005; Gallagher et al., 2011). Gallagher et al. (2011) applied a mobile digital imaging system which

\* Corresponding author.

E-mail addresses: [bas.huisman@deltares.nl](mailto:bas.huisman@deltares.nl) (B. Huisman), [M.A.deSchipper@tudelft.nl](mailto:M.A.deSchipper@tudelft.nl) (M. Schipper), [B.G.Ruessink@uu.nl](mailto:B.G.Ruessink@uu.nl) (B. Ruessink).

derived  $D_{50}$  from 2D autocorrelation of macro images of the surface sediment (Rubin, 2004).

The impact of storm conditions at natural coasts consists of a coarsening of the sediment grain size. Most prominent coarsening of the median grain diameter ( $D_{50}$  up to 100  $\mu\text{m}$  coarser) during a storm event with  $H_{m0} = 4$  m was observed in the swash zone (Stauble and Cialone (1996)). This coarsening gradually decreases in the offshore direction. Terwindt (1962) observed a quite uniform coarsening of  $\sim 30$   $\mu\text{m}$  from 2 to 15 meter water depth at the coast of Katwijk (The Netherlands) after a moderate summer storm ( $H_{m0} \sim 2$  m). Numerical modelling of cross-shore transport sorting during storms also shows coarsening of the nearshore zone and subsequent fining of the offshore sediment at the toe of the deposition profile (Reniers et al., 2013; Sirks, 2013; Broekema et al., in press). Seasonal variability of the cross-shore distribution of the grain size was observed by Medina et al. (1994), who shows that nearshore bed composition is coarsening in winter ( $H_{m0, \text{winter}} = \sim 4$  m) and restoring to a finer bed composition in summer ( $H_{m0, \text{summer}} = \sim 1$  m). The largest annual variability in the measured  $D_{50}$  was observed in the swash zone (up to 200  $\mu\text{m}$ ) at mean sea level (MSL) which gradually decreases to a variability of  $\sim 20$   $\mu\text{m}$  at MSL  $-8$  m. Seasonal variability of the  $D_{50}$  was, however, found to be almost negligible for a nourishment at the Dutch barrier island of Terschelling (Guillén and Hoekstra, 1996). Guillén and Hoekstra (1996) observed an 'equilibrium distribution' of the size fractions, which means that the cross-shore bed composition of each size fraction will be restored over time by the hydrodynamic processes to the natural equilibrium situation. An influence of the width of the littoral zone (which depends on the wave conditions) on the location of transitions in the cross-shore spatial variability in  $D_{50}$  of the sediment was suggested by Guillén and Hoekstra (1997).

The impact of the wave-driven longshore current on the along-shore heterogeneity of the bed composition was investigated by McLaren and Bowles (1985) with a focus on the changes of the sediment grain size distribution (size, standard deviation and skewness) along the transport path. A coastal section down-drift from a cliff was studied by McLaren and Bowles (1985) as well as some riverine cases. McLaren and Bowles (1985) observed two typical spatial patterns of changes of the grain size distribution in the direction of the transport, which were either finer, better sorted and more negatively skewed (abbreviated as FB–) or coarser, better sorted and more positively skewed (CB+). Other studies do, however, suggest that only a better sorting provides a consistent proxy for the pathways of the sediment (Gao and Collins, 1992; Masselink, 1992). The alongshore gradients in the  $D_{50}$  were generally quite small at the Rhone Delta ( $\sim 10$   $\mu\text{m}$  per kilometer; Masselink, 1992) and therefore seldom larger than the natural variability of the  $D_{50}$  (Guillén and Hoekstra, 1997). In general it can be stated that the literature on the impact of the littoral drift on the spatial variability of the bed composition is scarce, which holds especially for cases with large-scale interventions where sand is expected to diffuse alongshore.

The geological history (e.g. presence of former river bed deposits) also influences the spatial heterogeneity of the local bed composition but at a very large time-scale (millenia or longer; Van Straaten, 1965; Eisma, 1968). The geological situation is therefore often seen as an initial condition of the bed which determines the mean bed composition in the region (Medina et al., 1994; Guillén and Hoekstra, 1996). In general it can be stated that the relevance of the geological history is largest in areas where hydrodynamic forcing conditions are weaker (e.g. at deeper water) and subsequently the time scale of sediment redistribution is long (i.e. months to years).

Spatial variability of the grain size (on cross-shore profiles or alongshore) is often the result of differences in the behaviour of sediment grain size fractions for the same hydrodynamic forcing conditions (Richmond and Sallenger, 1984) which takes place at the spatial scale of sediment grains. A differentiation can be made in sorting due to transport, suspension and entrainment of the grains

(Slingerland and Smith, 1986). The transport sorting process is induced by the difference in magnitude of the transport for fine and coarse size fractions (Steidtmann, 1982). A larger proportion of the finer size fraction is transported away from an erosive coastal section than of the coarser size fractions. Differences in sediment fall velocity may for specific situations induce suspension sorting (Baba and Komar, 1981). The spatial scale of the area over which sediment is deposited is larger for smaller grains. Additionally the difference in the weight and size of the particle may induce preferential entrainment of the finer sand grains for regimes that are close to the critical bed shear stress of the sand (Komar, 1987). These processes may act together and induce a 'preferential transport' of (fine) sediment size fractions at locations where substantial gradients in the hydrodynamic forcing conditions are present. It is envisaged that the 'Sand Motor' nourishment (Stive et al., 2013) provides an ideal case study site to investigate these processes given the large gradients in wave energy and longshore transport.

The objective of this work is to investigate the spatial heterogeneity of the surface bed composition, with a focus on the median grain size ( $D_{50}$ ), at the large-scale 'Sand Motor' nourishment (Stive et al., 2013). Sediment sampling surveys were carried out at the Sand Motor shoreface and related to modelled hydrodynamic forcing conditions (i.e. mean and maximum bed shear stresses). Both (half-)yearly and bi-weekly measurements were carried out to assess the bed composition changes at annual and storm time scales.

## 2. Study area

The 'Sand Motor' nourishment was constructed on the southern part of the Holland coast (the Netherlands) between April and August 2011 with the aim of providing a 20-year buffer against coastal erosion (Stive et al., 2013). A total of 21.5 million  $\text{m}^3$  of sediment was dredged for the creation of two shoreface nourishments and a large peninsula of 17 million  $\text{m}^3$  (de Schipper et al., 2016). The planform design of the Sand Motor comprised of a hook-shape with a dune lake and open lagoon on the northern side (Fig. 1). The alongshore extent of the Sand Motor was initially about 2.5 km. The emerged part of the Sand Motor was about 1 km wide at the Sand Motor peninsula (i.e. measured at MSL with respect to the original coastline). The initial submerged cross-shore profile slope at the center of the Sand



Fig. 1. Aerial photograph of the Sand Motor after completion (September 2011). Note the clouds of fine-grained material moving to the North. Picture courtesy of Rijkswaterstaat/Joop van Houdt.

Motor was about 1:30 and extended up to MSL –10 m (de Schipper et al., 2016). This was considerably steeper than the cross-shore profile before construction of the Sand Motor which was characterized by an average beach slope which ranged from 1:50 in shallow water (up to MSL –4 m) to 1:400 (beyond MSL –10 m).

The hydrodynamics, morphology and sediment composition of the Sand Motor were monitored extensively after its implementation. This consisted of in-situ measurements such as bathymetry surveys (with 1 to 3 month intervals), (half-)yearly sediment sampling and measurements of hydrodynamic forcing conditions (e.g. using ADCPs and directional wave buoys). The bathymetry surveys show that sediment was redistributed from the Sand Motor peninsula to the adjacent coast (Fig. 2), which resulted in a transition from the initial blunt shape to a smooth planform shape. Erosion of ~1.8 million m<sup>3</sup> was observed at the peninsula in the first 18 months (de Schipper et al., 2016). Substantial accretion was especially observed during the first winter months after construction. A large spit was formed at the northern side of the Sand Motor, which partially blocked the lagoon entrance. From the following spring and summer onward the changes became more moderate as the nourishment evolved further and wave conditions became milder. It is noted that even after the first years the Sand Motor remained a large coastal disturbance. The nearshore bathymetry at the Sand Motor is characterized either by sections with a longshore uniform bar-trough system or transverse bars.

The sediment composition of the Sand Motor was measured during construction and had an average  $D_{50}$  of ~278  $\mu\text{m}$ . Beach and dune sediment of the adjacent coast generally consisted of fine sands (100 to 200  $\mu\text{m}$ ), while moderate sized sand was found in the swash and surf (200 to 400  $\mu\text{m}$ ) and finer sands in the offshore direction (100 to 300  $\mu\text{m}$ ) till 8 to 10 meter depth (Van Straaten, 1965; Janssen and Mulder, 2005). However, patches with coarse material (i.e. > 500  $\mu\text{m}$ ) can occasionally be found in deeper water North of the Sand Motor (Wijsman and Verduin, 2011).

The Holland coast wave climate is characterized by wind waves which originate either from the South-West (i.e. dominant wind direction) or the North-West (i.e. direction with largest fetch length). The wave climate is characterized by average significant wave heights at offshore stations of about 1 m in summer and 1.7 m in winter (Wijnberg, 2002) with typical winter storms with wave heights ( $H_{m0}$ ) of 4 to 5 m and a wave period of about 10 s (Sembiring et al., 2015). The most severe storms originate from the North-West and coincide with storm surges of 0.5 to 2 m. Storms from the South-West induce either a small storm surge or set-down of the water level of some decimeters. Offshore wave data are available in the present study at an offshore platform ('Europlatform') at 32 m water depth.

The tidal wave at this part of the North Sea is a progressive wave with largest flood velocities occurring just before high water. The mean tidal range is about 1.7 m at the nearby port of Scheveningen, while the horizontal tide is asymmetric with largest flow velocities towards the North during flood (~0.7 m/s) and a longer period with ebb-flow in southern direction (~0.5 m/s; Wijnberg, 2002). Tidal flow velocities at the Sand Motor peninsula are enhanced as a result of contraction of the flow (Radermacher et al., 2015).

### 3. Methodology

#### 3.1. Sediment sampling

Field surveys of bed sediment composition were carried out before, during and after construction of the Sand Motor over a time-frame of 4 years (Table 1) with the aim of assessing both the short-term (i.e. weekly) and long-term (i.e. annual) changes of the median grain size at the Sand Motor. Surfzone and shoreface sediment samples were collected at multiple cross-shore transects with a Van Veen grab sampler (Fig. 3).

Sediment sampling was performed on cross-shore transects spaced about 500 to 1000 m apart in the alongshore direction (Fig. 3). A higher sampling resolution was obtained in the cross-shore direction than alongshore, since bed composition is generally more variable in the cross-shore direction (Van Straaten, 1965). Typically about 5 to 12 samples were taken for each transect at 1 to 10 m below MSL and a few samples on the dry beach (typically in the swash zone). In this research the inter-comparison of the sediment data took place for pre-selected transects (A, B, D, E, F and G). Unfortunately sample transects for surveys T0, T2 and T4, which were collected within a different monitoring programme by Imares, were not co-located and therefore require interpolation of data from nearest transects (especially relevant for transect B).

The dry beach and swash zone samples were collected from land during low water. Sampling at the other locations took place from a ship. Nearshore points (up to MSL –2 m) were sampled during high tide, since sufficient water depth was needed for the vessel to navigate. The ship GPS was used to precisely navigate to the predefined location of each sample. The local water depth at the sample location was read from the onboard Sonar. A stainless steel Van Veen grab sampler with clam-shell buckets with a radius of about 15 cm was applied for the sampling. It is lowered by hand on a rope in open position and closes when it hits the bed. A layer of 5 to 10 cm of the top-layer of the bed is then excavated when the rope is pulled. The full samples were stored in labeled bags.

Some of the surveys aimed at specific goals. Three samples were collected at every location during the T3 survey to assess the impact

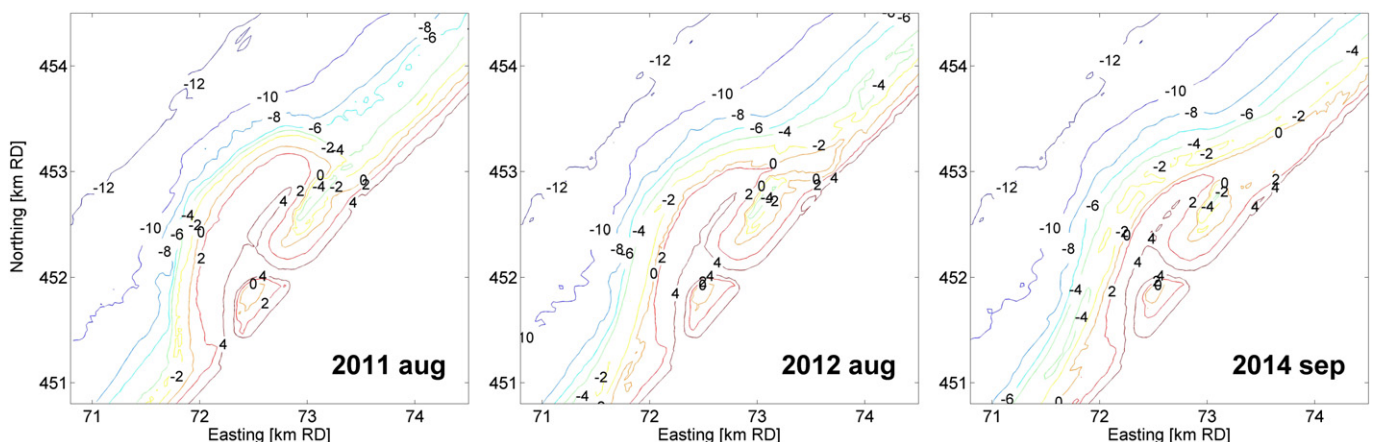


Fig. 2. Sand Motor bathymetry directly after construction (left), after 1 year (middle) and after 3 years (right).



**Table 1**  
Overview of bed composition surveys at the Sand Motor.

ID	Date	Executed by	Number of Transects	Samples per transect	Total number of samples <sup>*1</sup>	Repetition of sampling
T0	Oct' 2010	IMARES	6	6–8	42	1 ×
T1	Apr'–Nov' 2011	Contractor	– <sup>*2</sup>	– <sup>*2</sup>	25	1 ×
T2	Aug' 2012	IMARES	6	11–12	67	1 ×
T3	Feb' 2013	Delft university	6	7–10	165 <sup>*3</sup>	3 × in 1 survey
T4	Oct' 2013	IMARES	12	6–	93	1 ×
T5	Feb' 2014	Delft university	7	9–25	144	1 ×
T6	Sep'–Oct' 2014	Delft university	4	11–21	111	4 × bi-weekly <sup>*4</sup>

<sup>\*1</sup> Only the sample locations between MSL and MSL –10 m.

<sup>\*2</sup> T1 sample locations were scattered over the dry beach of the Sand Motor.

<sup>\*3</sup> Each location was sampled three times (i.e. 3 × 55 samples).

<sup>\*4</sup> The transect at the center of the Sand Motor peninsula was sampled four times over a period of six weeks.

of the sediment analysis method (mechanical sieving or Laser diffraction) on the obtained median grain diameters. Cross-shore gradients in the bed composition were assessed on the basis of detailed transects during the T5 survey (typically about 25 m to 30 m resolution between samples). Small timescale variations were measured during the T6 survey on a single transect at the center of the Sand Motor (i.e. transect D in Fig. 3), which was measured bi-weekly over a period of 6 weeks.

### 3.2. Sieving and treatment of sediment samples

The analysis of the grain size distribution of the samples was performed with a Laser diffraction device ('Malvern'; Weber et al., 1991) for the T0, T2 and T4 surveys and with mechanical sieving for the other surveys. The dry sieving method was applied according to BS812 (1975) standards. Wet sieving and pre-treatment with acid were applied for a selection of the T3 samples, which was relevant for a few samples North of the Sand Motor with a small but significant silt content. Either wet or dry sieving of these samples did,

however, have a negligible impact on the transect-averaged parameters used in this research. The weight percentiles of the full grain size distribution were determined. Derived properties of the grain size distribution such as the graphical sample standard deviation ( $\sigma_I$ ) and graphical skewness ( $Sk_I$ ) (Folk and Ward, 1957) were computed from the  $\phi$  values of the sediment (where  $\phi = -\log_2(D)$ , with  $D$  being the grain diameter in millimeters).

#### 3.2.1. Transect-averaged median grain size

A weighted average of the median grain size per cross-shore transect (referred to as  $D_{50TR}$ ) was used to analyse the alongshore spatial heterogeneity of the bed. The  $D_{50TR}$  is defined as follows:

$$D_{50TR} = \frac{1}{L} \sum_{i=1}^n D_{50,i} \Delta x_i \quad (1)$$

The contribution of each sample (landward of the MSL –10 m contour) is computed by multiplying the median grain size of the sample ( $D_{50,i}$ ) with the representative cross-shore extent ( $\Delta x_i$ , i.e.

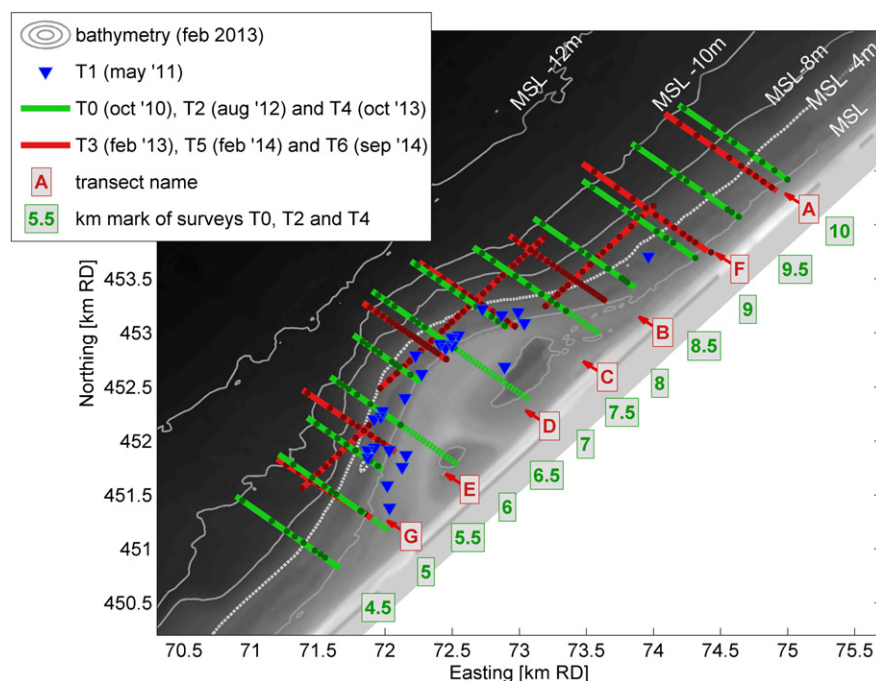


**Fig. 3.** Overview of sample locations for the seven field measurement surveys and the labeling of transects. Approximate locations for the T4 and T5 survey are presented as coloured dots on the transect lines. Note that part of the samples of the pre-construction survey T0 were collected at the location of the Sand Motor (dashed green lines). The de-linication between offshore and nearshore samples (as used in this research) is made at the MSL –4 m contour (i.e. white dashed line). (For interpretation of the references to colour in this figure legend, the reader is referred to the web version of this article.)

half of distance to neighboring sample). The summed  $D_{50}$  contribution of each sample is divided by the length of the considered transect ( $L$ ). Similarly, a transect-averaged median grain size was computed for the nearshore and offshore part of the cross-shore profile (respectively  $D_{50TR,ns}$  and  $D_{50TR,off}$ ) to examine alongshore heterogeneity at different sections of the cross-shore profile. The offshore and nearshore part of the profile were demarcated by the MSL –4 m contour (Fig. 3).

### 3.2.2. Inter-relation of laser diffraction and mechanical sieving

A correction was applied to the Laser diffraction (LD) sample data to make them comparable to mechanical sieving data, since the Laser diffraction analysis typically provides larger  $D_{50}$  values for the same samples (e.g. Konert and Vandenberghe, 1997). This correction was based on a linear fit of the median grain diameter determined using the T3 survey which was both analysed with Laser diffraction and mechanically sieving. The correction function reads as follows:

$$D_{50,sieve} = 0.899 * D_{50,LD} + 10.06 \quad (2)$$

The available  $D_{50}$  measurements of the T3 survey and linear fit ( $R^2$  of 0.89) are presented in Fig. 4. Similar relations were applied by Rodríguez and Uriarte (2009) and Zonneveld (1994).

### 3.2.3. Uncertainty in sampling and analysis methodology

The T3 survey data with mechanically sieved and corrected Laser diffraction samples provided a proxy for the accuracy of the analysis methodology. The standard deviation of the  $D_{50}$  of the difference between the corrected Laser diffraction samples and mechanically sieved samples (of the same physical samples) was 12  $\mu\text{m}$  (Fig. 4) and is considered a quantification of the uncertainty in the  $D_{50}$  due to the analysis methodology. Similarly, also the difference between two mechanical sieved data sets (from the same T3 samples) was determined which was 15  $\mu\text{m}$  ( $R^2$  of 0.83). The inaccuracy in the sampling method was considered similar for mechanical sieving or Laser diffraction analyses. An estimate of 30  $\mu\text{m}$  (i.e.  $2 \times \text{STD}$  of the mechanically sieved sample sets) was therefore made for the 95% confidence interval in the mechanical sieving or Laser diffraction analysis. The inaccuracy of  $D_{50TR}$  was also determined from the considered data sets (for Laser diffraction and mechanical sieving) which was considerably smaller than for the individual samples. The 95% confidence interval of the  $D_{50TR}$  was found to be  $\pm 11 \mu\text{m}$  on the basis of a re-analysis of the T3 survey with a Laser diffraction device.

### 3.3. Climate conditions

Time-series of wave conditions for the T0 to T6 surveys were derived from the 'Europlatform' measurement station (see wave

height and wave direction in Fig. 5). The wave conditions were considered typical for the Dutch coast (Wijnberg, 2002) with an average significant wave height ( $H_{m0}$ ) of 1.1 m for all considered survey periods. Considerable temporal variation in the magnitude and direction of the waves was, however, observed for the period of the measurements and preceding month. Sampling of the sediment typically took place during quiet and moderate wave conditions ( $H_{m0}$  from 0.3 to 1.5 m with an average  $T_{m02}$  of about 4 s). Occasional storm events (i.e. offshore wave height from 3 to 5.4 m) were observed both in the winter and summer surveys. The largest storm event in the considered survey periods was observed on 22 October 2016 (during T6 survey). This event had an offshore significant wave height ( $H_{m0}$ ) of about 5 m and originated from the North-West ( $\sim 310^\circ \text{N}$ ). It is noted that the T2 survey measurements were taken only a few days after a storm event on 25 and 26 August 2012 (offshore  $H_{m0}$  of 3.3 m) which approached the coast from the West ( $\sim 263^\circ \text{N}$  at MSL –8 m). This storm followed a month with relatively quiet conditions.

### 3.4. Hydrodynamic modelling

In this research we explored how observed bed composition changes relate to local hydrodynamic forcing conditions at the Sand Motor. For this purpose a Delft3D model (Lesser et al., 2004) was setup to hindcast wave and tide conditions at the Sand Motor. The Delft3D model applies the shallow water equations for the flow computations. The wave energy transport model SWAN was used for the wave modelling (Booij et al., 1999). The model domain includes the Sand Motor and adjacent coast (Fig. 6). Time-series of wave conditions were derived from the 'Europlatform' wave measurement station for each of the survey periods. Tide conditions were derived from an operational model for the North Sea (CoSMoS, Sembringpress et al., 2015) and applied on the boundaries of the model. The modelled hydrodynamics were validated by Luijendijk et al. (in press) by means of a comparison with wave measurements at a nearshore wave buoy and current velocities at two ADCP stations. These comparisons showed that nearshore waves and tidal flow velocities were well predicted. Detailed settings of the model are described by Luijendijk et al. (in press). Bed shear stresses as a result of currents and waves ( $\tau_{cw,mean}$  and  $\tau_{cw,max}$ ) were computed with the method of Van Rijn et al. (2004) (Appendix A).

A hindcast of the wave and tide conditions was made for the month preceding each of the surveys (T0 to T6) using the most recently surveyed bathymetry. A time-series of a full month was used to make sure that both normal and storm conditions are included. The time-series of  $\tau_{cw,mean}$  and  $\tau_{cw,max}$  were averaged over the considered month at every grid-cell to obtain a spatial field of time-averaged mean and maximum bed shear stresses. These time-averaged bed shear stresses ( $\bar{\tau}_{cw,mean}$  and  $\bar{\tau}_{cw,max}$ ) were then correlated to the  $D_{50TR}$  at predefined cross-shore transects of the surveys.

## 4. Sediment survey data

Short-term temporal and spatial variability of the bed sediment composition at the Sand Motor peninsula was investigated on the basis of the T6 survey measurements. The observed short-term temporal variability of the  $D_{50}$  during the T6 survey provided a proxy for the short-term temporal variability of the  $D_{50}$  in the half-yearly bed sediment surveys at the Sand Motor (T0 to T6).

### 4.1. Short-term variability of bed sediment composition

Cross-shore bed sediment composition at the center of the Sand Motor (transect D) was quite similar for the different measurement occasions of the T6 survey (Fig. 7). The sediment at transect D was typically medium sand. All measurements contained a peak

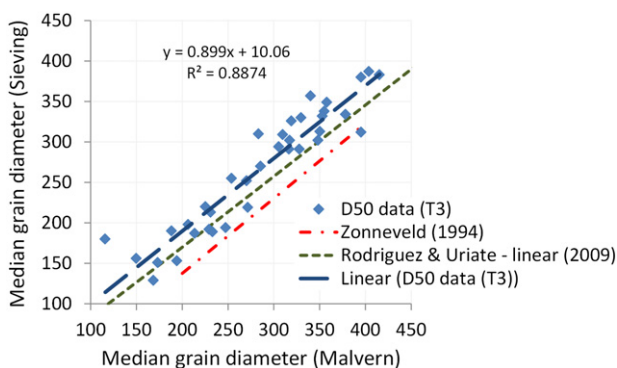
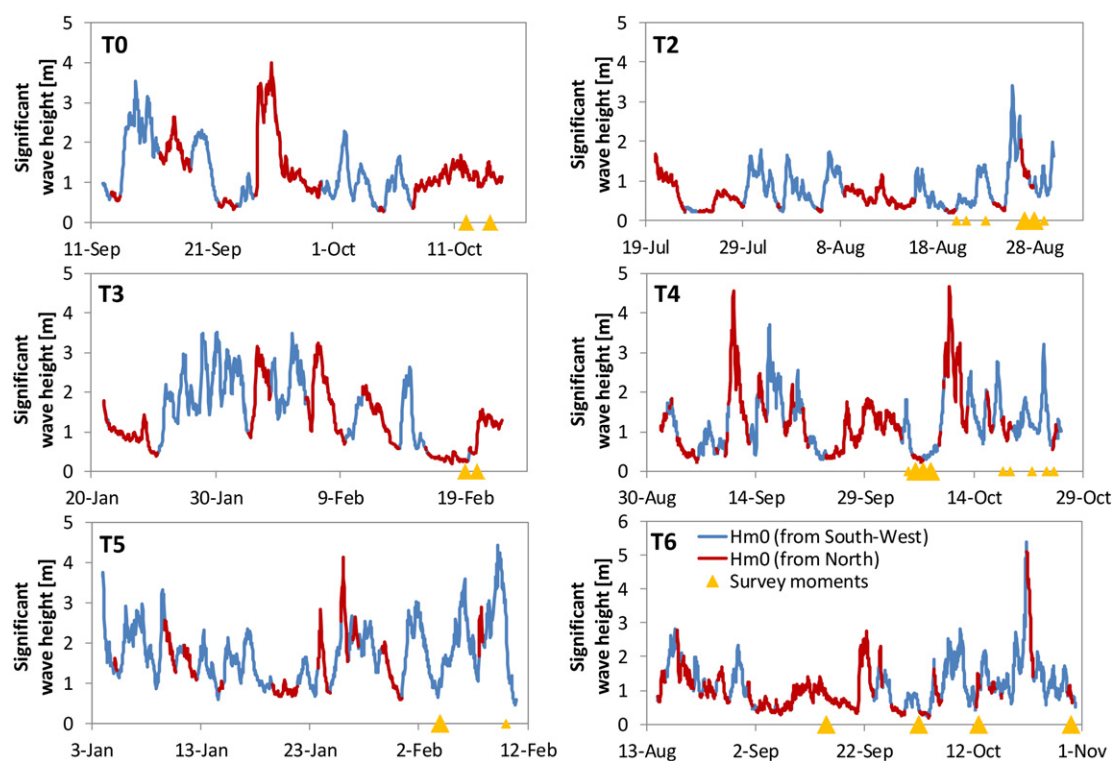


Fig. 4. Re-analysis of  $D_{50}$  of T3 survey with Laser diffraction and Mechanical sieving and resulting correction factor.



**Fig. 5.** Offshore significant wave height ( $H_{m0}$ ) at 'Europlatform' measurement station for the surveys T0 and T2 to T6 (and preceding month). The blue and red line colours indicate the waves originating from the West ( $< 312^\circ\text{N}$ ) or North ( $> 312^\circ\text{N}$ ). Larger survey markers represent moments at which most of the surfzone samples were collected. (For interpretation of the references to colour in this figure legend, the reader is referred to the web version of this article.)

with coarser sand ( $D_{50}$  of about 370 to 420  $\mu\text{m}$ ) in the bar trough,  $\sim 300 \mu\text{m}$  sediment on the seaward side of the bar in intermediate water depths (from MSL  $-3 \text{ m}$  to MSL  $-5 \text{ m}$ ) and 320 to 370  $\mu\text{m}$  sand

in deeper water. The transect-averaged  $D_{50}$  ( $D_{50\text{TR}}$ ) of transect D of the T6 survey was on average 331  $\mu\text{m}$ , while  $D_{50\text{TR,off}}$  and  $D_{50\text{TR,ns}}$  were respectively 338 and 320  $\mu\text{m}$  for this transect.

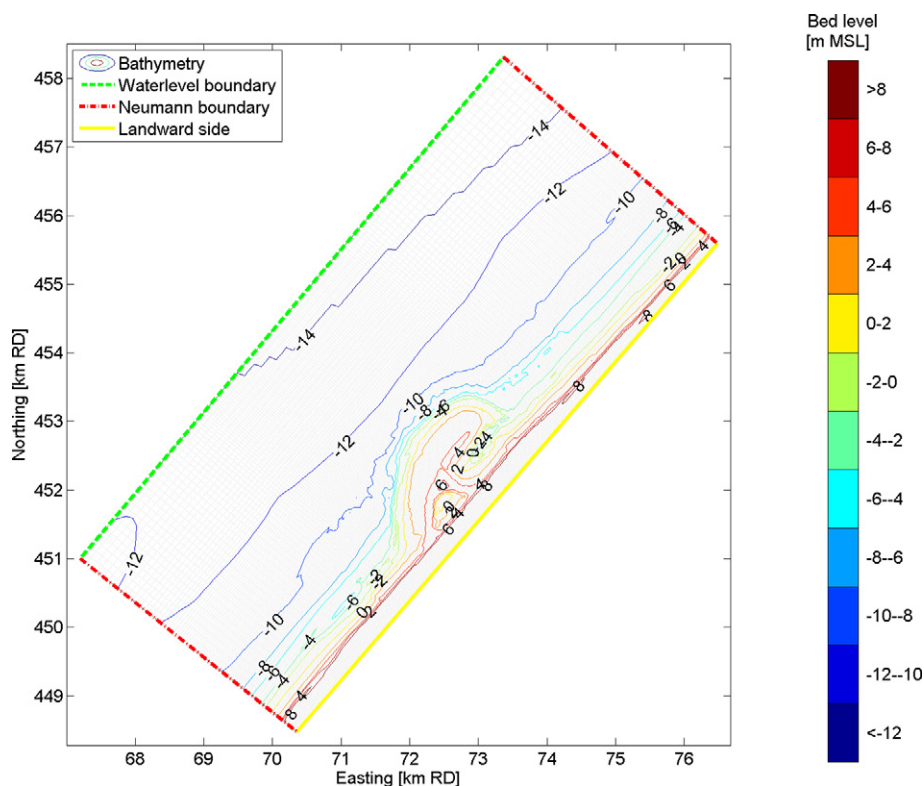


**Fig. 6.** Model domain with initial Sand Motor bathymetry of August 2011 and boundary conditions.

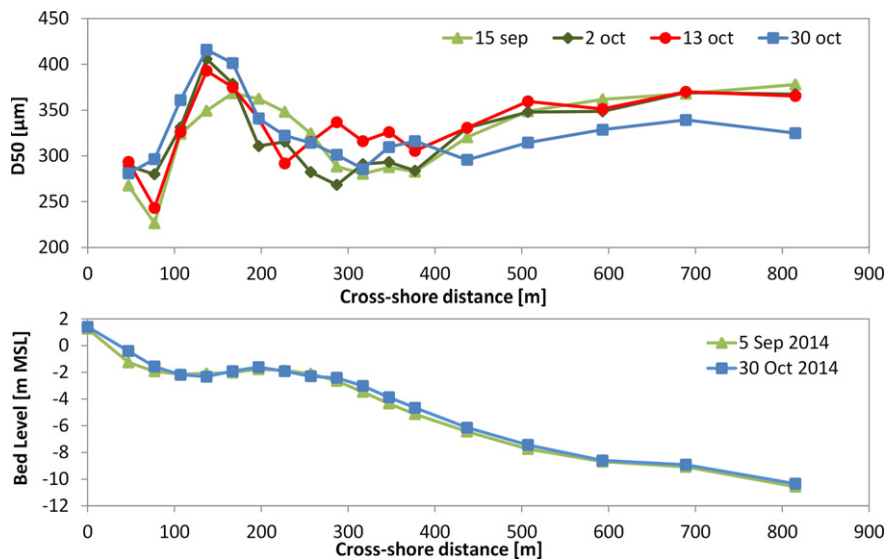


Fig. 7. Measured median grain diameter ( $D_{50}$ ) and bed level at transect D of the T6 measurement survey (i.e. center of Sand Motor).

The most significant change in the bed composition consisted of a finer  $D_{50}$  of 30 to 40  $\mu\text{m}$  at deeper water (from MSL –6 m to MSL –11 m) in the October 30 measurements, which was a post-storm survey after the October 22 storm. The transect-averaged bed composition ( $D_{50\text{TR}}$ ) was slightly finer for the October 30 measurements with a  $D_{50\text{TR}}$  of 325  $\mu\text{m}$ . The grain size distribution of the bed between MSL –6 m and MSL –8 m became more fine skewed ( $Sk_I$  of +0.2) in the October 30 measurements and more coarse skewed ( $Sk_I$  of –0.2) in the trough of the bar. This is in contrast with the other measurement occasions of the T6 survey for which a very small  $Sk_I$  was observed (Appendix B). Bed composition changes in the nearshore consisted of a wider and less pronounced peak with coarser bed material in the first survey (September 15), which was preceded by low northerly waves. Coarsening of the bed took place between the 2nd and 13th of October measurements at the seaward side of the sub-tidal bar (from MSL –2 m to MSL –5 m) after a period with dominant wave conditions from the West ( $H_{m0}$  up to 2.8 m).

The variability of the bed sediment composition in time was expected to be the result of the hydrodynamic conditions given the considerable (permanent or temporary) change in  $D_{50}$  after the October 22 storm, which is also in line with observed temporal variability in  $D_{50}$  by Stauble and Cialone (1996). Changes in  $D_{50}$  during the short-term T6 measurements are considered a proxy for the temporal variability of  $D_{50}$  as a result of hydrodynamics in other sediment sampling surveys at the Sand Motor, which also experienced similar normal conditions and a severe storm (Fig. 5). The average significant wave height of the T6 survey was equal to the average of all surveys ( $H_{m0,\text{off}} = 1.2$  m), while the storm was more severe during the T6 survey than for the other surveys ( $H_{m0,\text{off}} = 5.4$  m during the T6 survey and an average  $H_{m0,\text{off}} = 4$  m for the other surveys). The intra-survey variability was quantified as  $2 \times$  the standard deviation of the variability in  $D_{50}$  of individual sample locations throughout the six week period of the T6 survey. This amounts to an estimate of 40  $\mu\text{m}$  for the uncertainty in  $D_{50}$  of individual samples and 10  $\mu\text{m}$  for  $D_{50\text{TR}}$ . The variability in the nearshore and offshore averaged median grain diameters ( $\Delta D_{50\text{TR,NS}}$  and  $\Delta D_{50\text{TR,OFF}}$ ) was respectively 16  $\mu\text{m}$  and 24  $\mu\text{m}$ .

#### 4.2. Long-term bed sediment composition changes

Bed sediment composition at the Sand Motor changed from a rather alongshore uniform bed composition (T0 survey) to a situation

with considerable alongshore heterogeneity in  $D_{50}$  over the entire four year study period (Fig. 8).

The pre-construction situation (T0; panel a in Fig. 8) was characterized by a fining of the sediment in the offshore direction. Typically a median grain diameter of about 300 to 400  $\mu\text{m}$  was found at the waterline and  $\sim 200$   $\mu\text{m}$  sand at MSL –7 m contour and deeper. The alongshore variability in sediment size is largest in shallow water (MSL –2 m) and decreases in the offshore direction, which is in line with other observations along the Holland coast (Wijnberg and Kroon, 2002). The standard deviation of the grain size distribution ( $\sigma_I$ ) ranged from 0.6 to 0.8 for most samples, with largest  $\sigma_I$  for samples that were collected seaward of MSL –5 m (Appendix B). Skewness ( $Sk_I$ ) ranged from –0.2 to 0.1 with slightly more positive skewness in shallow water (from MSL to MSL –3 m).

Sediment samples at the dry beach that were collected during the construction of the Sand Motor (T1; panel b in Fig. 8) typically had a median grain diameter ( $D_{50}$ ) between 250 and 310  $\mu\text{m}$  (278  $\mu\text{m}$  on average with  $\sigma_I$  of 30  $\mu\text{m}$ ). The relatively uniform bed at the dry beach was expected to be the result of mixing during the dredging and nourishing activities. Whether the underwater bed sediment was of similar composition is not known directly from measurements. It was expected that similar sand was used also offshore since the nourished material needed to adhere to the specifications with respect to grain size (i.e. between 200 and 300  $\mu\text{m}$ ). Suspension sorting (Slingerland and Smith, 1986) as a result of the dumping of the sediment may, however, have taken place. Consequently, some of the finest sand and silt fractions that were nourished may be missing from the underwater bed sediment of the Sand Motor.

The first survey after construction of the Sand Motor (T2; panel c in Fig. 8) did not show the gradual fining in the offshore direction. Instead coarser sediment was found in shallow water (landward of MSL –2 m) and deeper water (beyond MSL –6 m), while finer sand was found at intermediate depths along the western side of the Sand Motor (i.e. 100 to 200  $\mu\text{m}$  from MSL –4 m to MSL –8 m). Overall, the average bed sediment composition ( $D_{50}$ ) of the T2 survey was considerably coarser than the natural bed (T0 survey), as well as coarser than the sediment that was used for construction (T1 survey). The  $D_{50}$  landward of MSL –2 m typically was  $\sim 500$   $\mu\text{m}$ , while offshore  $D_{50}$  ranged from 300 to 500  $\mu\text{m}$ .

Considerably coarser sediment ( $D_{50}$ ) was observed at the central Sand Motor transects from about 1.5 years after construction of the



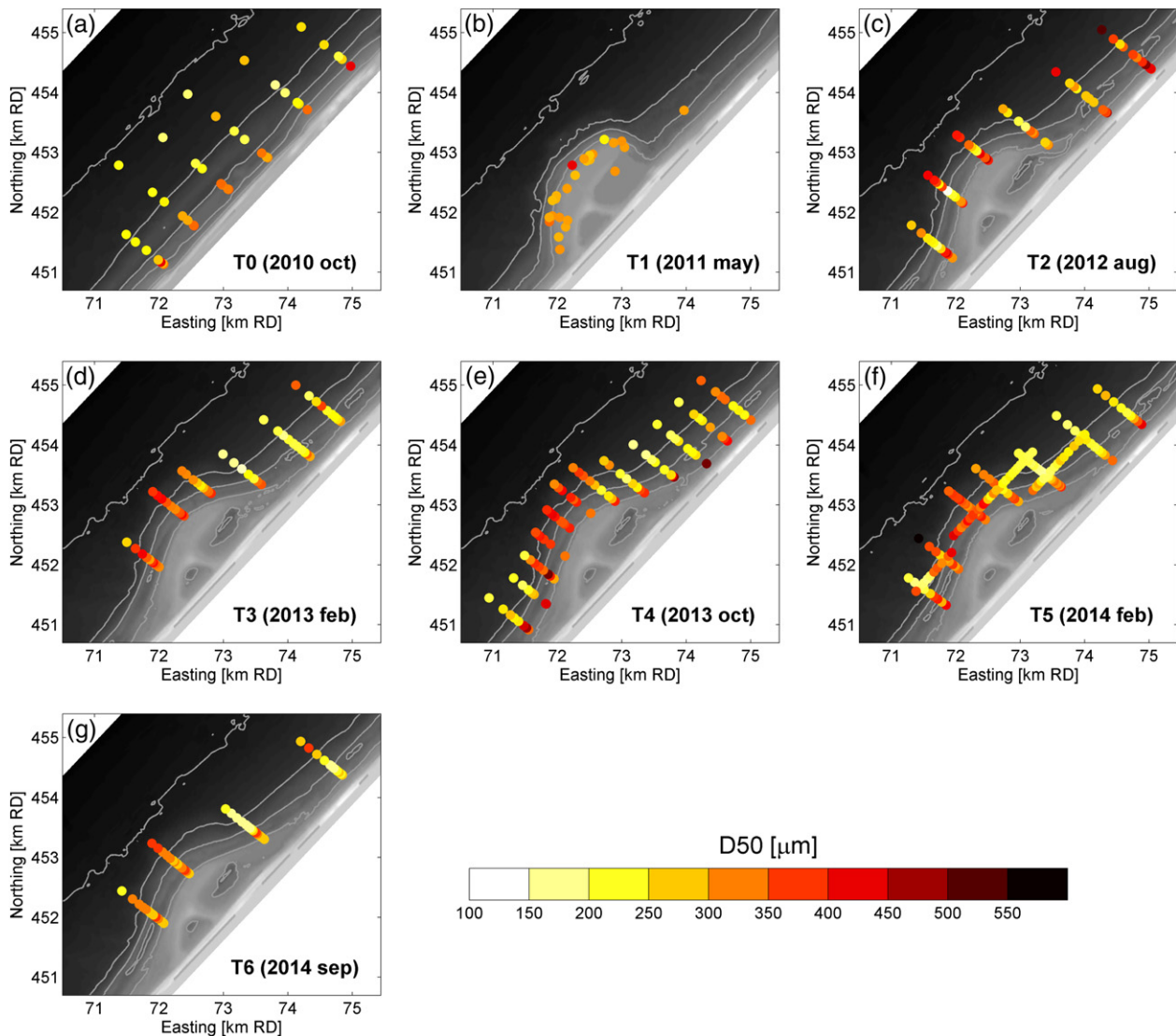


Fig. 8. Median grain diameter of sediment samples for T0 to T6 surveys (respectively a to g).

Sand Motor (i.e. surveys T3 to T6) and a fining of the bed at the Northern and Southern flanks (panel d to g in Fig. 8). This alongshore heterogeneity of the bed composition ( $D_{50TR}$ ; Appendix C) had a length scale which is similar to the size of the Sand Motor ( $\sim 2$  km; Fig. 9). The coarsening of the transect-averaged median grain diameter ( $D_{50,TR}$ ) at the central transects of the Sand Motor (transect D and E) was up to  $+140 \mu\text{m}$ , which was considerably coarser than the average  $D_{50,TR}$  of the T0 survey which was  $220 \mu\text{m}$ .  $D_{50,TR}$  was up to  $50 \mu\text{m}$  finer for the transects North of the Sand Motor (i.e. transects B and F). It is noted that a more extensive fining of the bed may have been present in the area North of the Sand Motor, but was possibly not captured by the sampling at the current transects.

The observed changes in  $D_{50TR}$  at the Sand Motor peninsula (transect D in Fig. 9) well exceeded the uncertainty as a result of the analysis methodology ( $\sim 11 \mu\text{m}$  for  $D_{50TR}$ ) and short-term temporal variability of the bed composition ( $\sim 10 \mu\text{m}$  for  $D_{50TR}$ ) as observed in the T6 survey. The alongshore heterogeneity of the  $D_{50}$  after construction of the Sand Motor was substantially larger than for the reference survey (T0) which had a relatively uniform spatial bed composition ( $-10\%$  to  $+5\%$  deviation of  $D_{50TR}$  from the survey average). From T3 onward, the grain size distribution at the center transects of the Sand Motor was relatively narrow ( $\sigma_I$  of 0.4 to 0.6)

compared to the grain size distribution of the nourished sediment, while more poorly sorted sand ( $\sigma_I$  of 0.7 to 0.9) was found in deeper water (from MSL  $-5$  m to MSL  $-10$  m) North and South of the Sand Motor area. The reduction of  $\sigma_I$  at the Sand Motor provides an indication for changes in bed composition as a result of hydrodynamic sorting processes (e.g. due to differences in transport gradients or entrainment of sediment size fractions).

#### 4.3. Cross-shore variability of $D_{50}$

A more detailed investigation into the cross-shore sediment distribution at the Sand Motor peninsula and adjacent coast, showed that the cross-shore distribution of  $D_{50}$  was rather uniform at the central Sand Motor transects ( $D_{50}$  from 300 to  $400 \mu\text{m}$  at transects D) when compared to the natural fining in the offshore direction that was observed in the reference survey T0 (Fig. 10). A natural fining of the sediment in the offshore direction was observed for the transects North and South of the Sand Motor (see example for transect B in Fig. 10). A quantification of the cross-shore variability of the  $D_{50}$  by means of a linear regression for all samples in the active zone (from MSL to MSL  $-8$  m) indicated an average cross-shore fining of  $\sim 24 \mu\text{m}$  per meter depth in the offshore direction ( $R^2 \geq 0.83$ ).



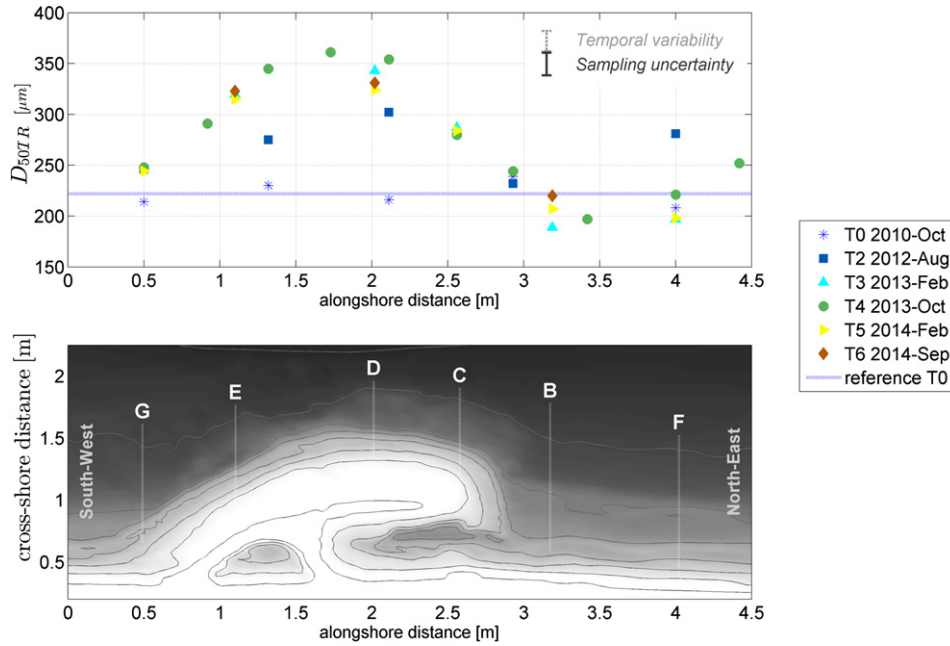


**Fig. 9.** Alongshore variability in the transect-averaged median grain diameter ( $D_{50TR}$ ) at the Sand Motor.

Alongshore heterogeneity of the bed composition was most prominent in deeper water seaward of the sub-tidal bar ( $D_{50TR,off}$  of +90 to +150  $\mu\text{m}$  with respect to T0 survey; Fig. 11) as a result of the relative coarse  $D_{50}$  in deeper water at the Sand Motor (Table C.1). In the nearshore the  $D_{50TR,ns}$  at the Sand Motor (transects D and E) was only moderately coarser than  $D_{50TR,ns}$  at the adjacent coastal sections (0 to +70  $\mu\text{m}$  coarser).

#### 4.4. Temporal development of $D_{50}$

The temporal variation of the bed composition at the Peninsula of the Sand Motor (transect D) consisted of an initial increase of the  $D_{50TR}$  at T1 from about 216 to 278  $\mu\text{m}$  during construction of the Sand Motor (Fig. 12, panel a) which was followed by additional coarsening of  $D_{50TR}$  from the T1 to T3 survey (up to ~340  $\mu\text{m}$ ). The observed  $D_{50TR}$  (at transect D) was more steady after survey T3 with a small tendency towards a reduction of the coarsening after the T4 survey. The  $D_{50TR}$  of transects North of the Sand Motor (B and F) were either similar or somewhat finer than for the T0 survey (0 to –50  $\mu\text{m}$  change compared to T0).

The gradual increase in the  $D_{50TR}$  at the Sand Motor peninsula in the first two years (from T1 to T4) exceeded the uncertainty as a

result of the analysis methodology and short-term temporal variability. Observed coarsening was therefore not considered due to initial construction of the Sand Motor alone, but partly also the result of a gradual process in time.

The longer-term behaviour of the  $D_{50TR}$  from survey T3 onward was much more subtle (Fig. 12) and therefore makes it difficult to discern a trend. This may partly be due to a seasonal influence on the  $D_{50}$  of the measurement surveys, which was perceived to be present at transects North of the Sand Motor (panel b in Fig. 12). These transects show ~30  $\mu\text{m}$  coarser surveys in summer (T4 and T6) than in winter (T3 and T5). In order to filter out the bias of the surveys (e.g. due to seasonality) it is therefore proposed to use the difference in the  $D_{50TR}$  between the coarsest and finest transect of each survey (respectively  $D_{50TR,max}$  and  $D_{50TR,min}$ ) with respect to the average  $D_{50TR}$  of each survey ( $\overline{D_{50TR}}$ ) as a proxy for the ‘degree of alongshore heterogeneity’ of the  $D_{50}$  ( $S_{alongshore}$ ). The  $S_{alongshore}$  is given by the following equation:

$$S_{alongshore} = \frac{D_{50TR,max} - D_{50TR,min}}{\overline{D_{50TR}}} \quad (3)$$

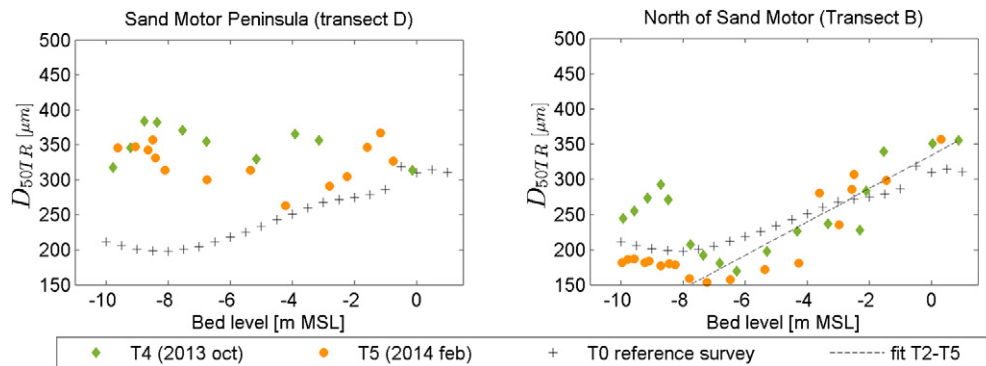


**Fig. 10.** Cross-shore distribution of  $D_{50}$  at the Sand Motor peninsula and adjacent coast (transects B and D) before and after construction of the Sand Motor for a representative summer and winter survey (T0, T4 and T5).

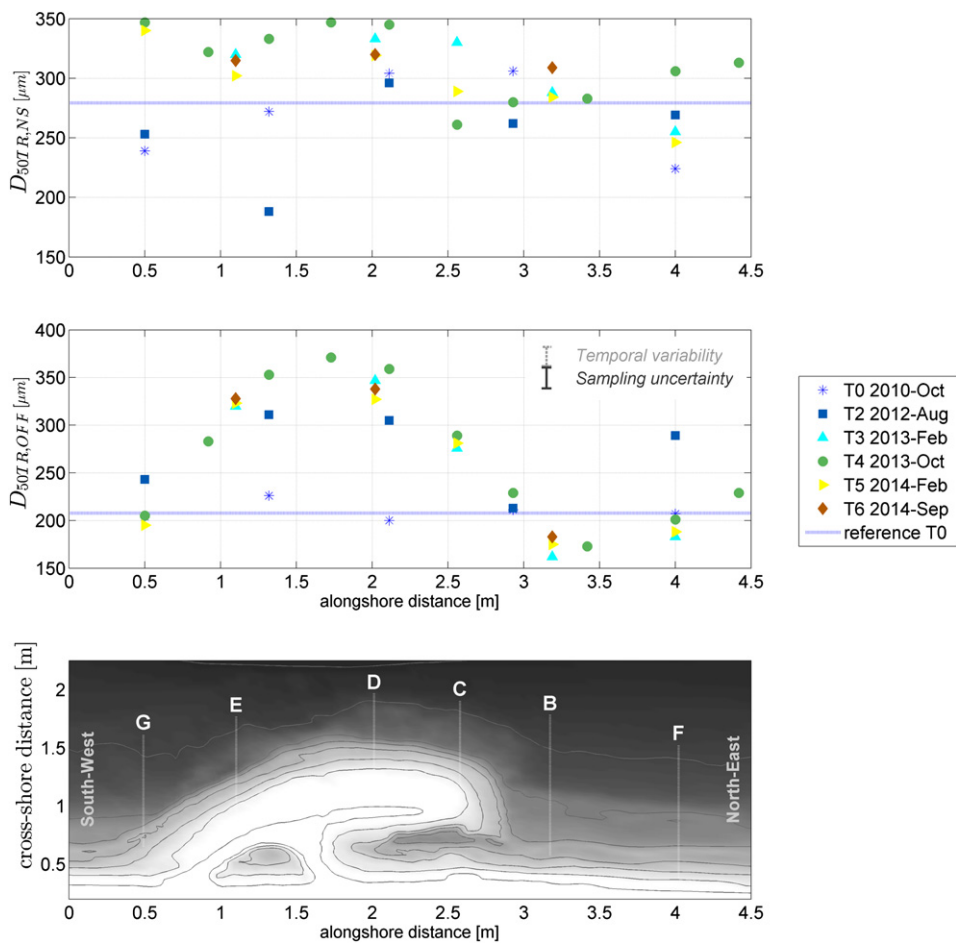


Fig. 11. Alongshore variability in the offshore and nearshore averaged median grain diameter ( $D_{50TR,NS}$  and  $D_{50TR,OFF}$ ) at the Sand Motor.

Long-term development of  $S_{alongshore}$  for transects B and D (i.e. finest and coarsest transect) shows a considerably enhanced degree of alongshore heterogeneity ( $S_{alongshore}$ ) compared to the natural alongshore variability in the T0 survey (Fig. 13). This  $S_{alongshore}$  decreased slowly over time since the T3 survey (~30  $\mu\text{m}$  decrease per year).

5. Inter-relation of alongshore heterogeneity of the  $D_{50}$  with bed shear stresses

An inter-comparison was made of the alongshore heterogeneity of the  $D_{50}$  (using the transect-averaged  $D_{50TR}$ ) with monthly averaged bed shear stresses as a result of waves and currents ( $\bar{\tau}_{cw,mean}$  and  $\bar{\tau}_{cw,max}$ ) with the aim to investigate what hydrodynamic conditions

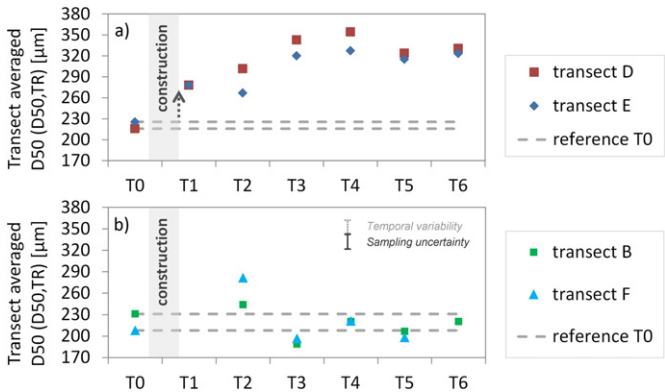


Fig. 12. Transect-averaged median grain diameter ( $D_{50TR}$ ) over time at the center of the Sand Motor (panel a) and North of the Sand Motor (panel b).

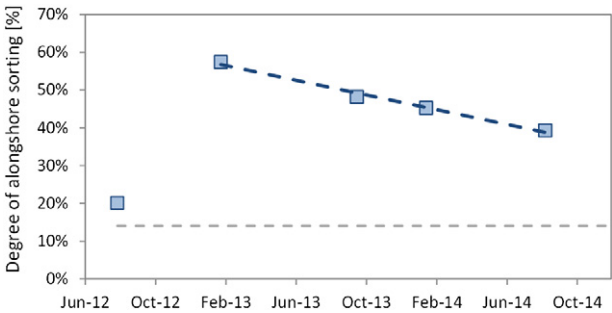


Fig. 13. Time development of the the degree of alongshore heterogeneity of the  $D_{50}$  ( $S_{alongshore}$ ) from the difference of transects B and D of surveys T2 to T6 [-] (with respect to  $D_{50TR}$ ). The average natural alongshore variability of the  $D_{50TR}$  for all transects of the T0 survey is shown with the dashed grey line.

(i.e. storm or normal conditions) are responsible for the observed large scale alongshore bed composition changes.  $\bar{\tau}_{cw,mean}$  is mainly influenced by the tide and moderate wave conditions, while the  $\bar{\tau}_{cw,max}$  is influenced predominantly by storm wave conditions. The typical summer and winter conditions are presented for October 2013 and February 2014 (i.e. T4 and T5 survey; Fig. 14).

The largest bed shear stresses were present along the shore-line as a result of the waves and wave-induced longshore current, which is most evident for the more energetic February 2014 conditions ( $\bar{\tau}_{cw,max}$  in Fig. 14d). Furthermore, a large area with enhanced bed shear stresses ( $\bar{\tau}_{cw,mean}$  ranging from 0.6 to 1 N/m<sup>2</sup>) was present in front of the Sand Motor as a result of tidal flow contraction (Fig. 14a), which had a similar magnitude for both winter and summer conditions. This area extends approximately from MSL –13 m till MSL –4 m and has an alongshore extent of about 2 km.

The observed spatial pattern of the  $\bar{\tau}_{cw,mean}$  is considered qualitatively similar to the observed spatial  $D_{50}$  distribution at the Sand Motor (Fig. 8). A positive relation between the transect-averaged mean bed shear stresses ( $\bar{\tau}_{cw,mean}$ ) and the transect-averaged median grain diameter ( $D_{50TR}$ ) was found for survey T4 (Fig. 15,  $R^2 = 0.8$ ), while no correlation was found with the maximum bed shear stresses ( $\bar{\tau}_{cw,max}$ ). Note that the T4 survey is shown here since it has the most cross-shore transects (i.e. better alongshore resolution).

Similar relations between  $D_{50TR}$  and transect-averaged bed shear stresses ( $\bar{\tau}_{cw,mean}$ ) were found for the other surveys (Fig. 16). A positive correlation was found for surveys T3, T5 and T6 (respectively  $R^2$  of 0.79, 0.65 and 0.64) and small correlation for the T2 survey ( $R^2$  of 0.3) which was preceded by a storm which followed

a period with relatively quiet conditions. The correlation between  $\bar{\tau}_{cw,mean}$  and  $D_{50TR}$  suggests that enhanced hydrodynamic forcing conditions (due to tidal flow contraction) induce a mechanism which contributes to the development of the alongshore heterogeneity of the bed composition ( $D_{50TR}$ ) at the Sand Motor.

The local increase in the mean bed shear stresses ( $\bar{\tau}_{cw,mean}$ ) at the Sand Motor is considered a relevant driver for the generation of large-scale alongshore heterogeneity of the  $D_{50}$  at the Sand Motor peninsula on monthly to annual time scales. The locally higher potential to suspend sediment results in alongshore transport away from the Sand Motor which mainly consists of the finer sand fractions (referred to as ‘preferential transport’). These finer sand fractions are mobilized more often than coarse sand fractions, because the thresholds for pick up of sand are more often exceeded as a result of the increased bed shear stresses. Van Rijn (1993) indicates a threshold value of  $\sim 0.4$  N/m<sup>2</sup> for suspension of 400  $\mu$ m sand. This critical bed shear stress is in the range of the average shear stresses in deeper water (seaward of MSL –4 m) of the Sand Motor (about 0.4 to 1 N/m<sup>2</sup>). The strong correlation of  $D_{50TR}$  with  $\bar{\tau}_{cw,mean}$  (which is dominated by the tidal current) suggests that the coarsening of the bed at the Sand Motor was influenced by a mechanism which coarsened the top-layer of the bed during normal conditions. The preferential transport of fine sand is expected to be responsible for coarsening in front of the Sand Motor peninsula from T1 to T3. The fining North and South of the Sand Motor is considered to be the result of the supply of relatively fine sand from the eroding sections of the Sand Motor.

A (partially) armored top-layer is expected to be present in front of the Sand Motor peninsula roughly between MSL –8 m

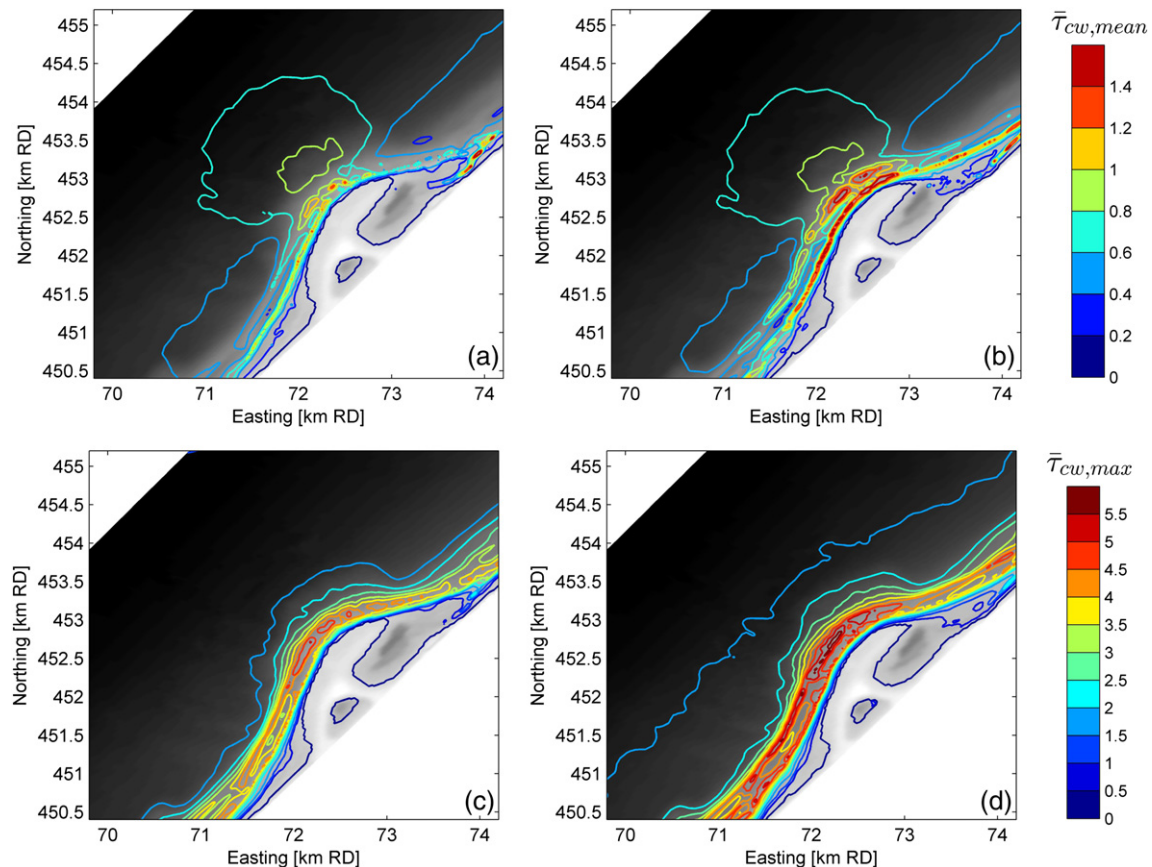


**Fig. 14.** Mean and maximum bed shear stresses averaged over a month for October 2013 (T4) and February 2014 (T5). Panel a:  $\bar{\tau}_{cw,mean}$  (October 2013); Panel b:  $\bar{\tau}_{cw,mean}$  (February 2014); Panel c:  $\bar{\tau}_{cw,max}$  (October 2013); Panel d:  $\bar{\tau}_{cw,max}$  (February 2014).



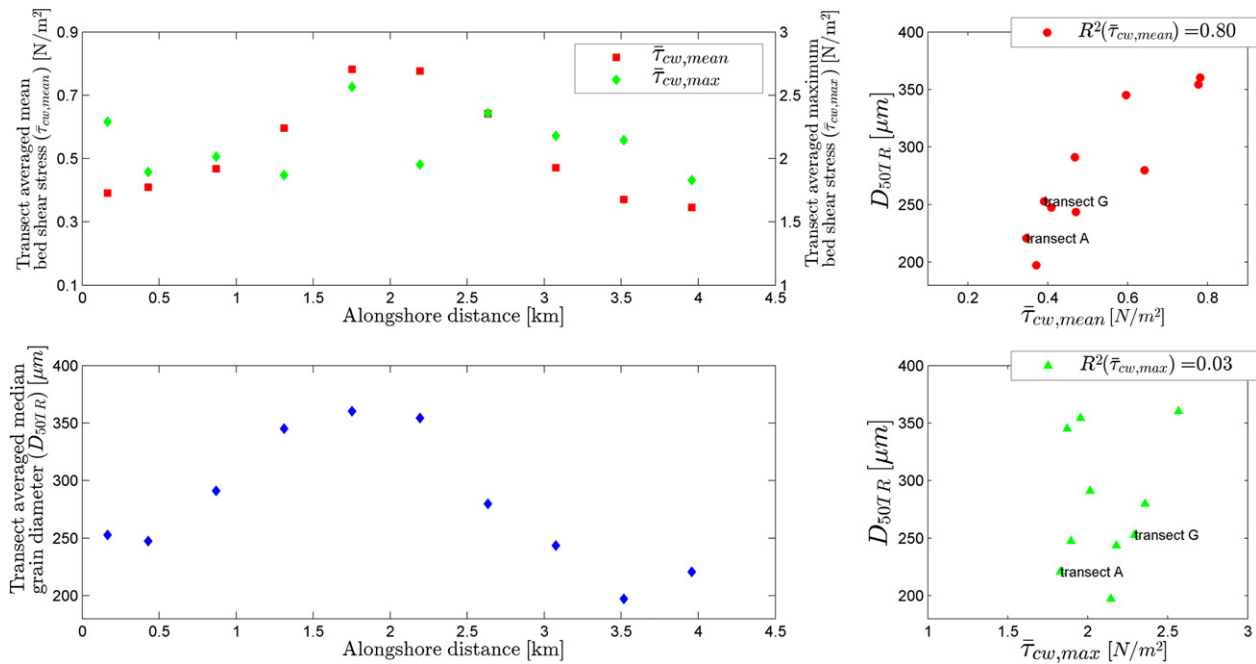


**Fig. 15.** Inter-relation between transect-averaged bed shear stress ( $\bar{\tau}_{cw,mean}$ ) and median grain diameter ( $D_{50TR}$ ) for the T4 survey transects. Top-left: Mean bed shear stress along the coast (using the same alongshore distance reference as Fig. 10). Lower-left:  $D_{50TR}$  along the coast. Top-right:  $\bar{\tau}_{cw,mean}$  versus  $D_{50TR}$ . Lower-right:  $\bar{\tau}_{cw,max}$  versus  $D_{50TR}$ .

and MSL –13 m as a result of the preferential transport/erosion of finer sand. This is in agreement with the observations of a narrower grain size distribution at the Sand Motor peninsula (standard deviation of the grain size distribution of  $\sim 0.5$  instead of 0.6 to 0.8 for the nourished material). The underlying substrate is, however, expected to be more poorly sorted as it is not yet affected by the hydrodynamic processes, which means that the fining of the Sand Motor during the October 22 storm (T6 survey) is most likely related to mixing of the top-layer sediment with the substrate. In short it is perceived that tidal flow contraction at the Sand Motor induces a mechanism of preferential transport which substantially affects the alongshore heterogeneity of the  $D_{50}$ .

## 6. Discussion

A number of contributors for bed composition changes at the Sand Motor were identified on the basis of the survey results and hydrodynamic modelling. The main contributors are 1) preferential transport of finer sand fractions during moderate conditions, 2) mobilization of coarse sand fractions and cross-shore transport during storm events and 3) the initial disturbance of the bed composition during construction.

### • I: Moderate conditions

Preferential transport of finer sand may take place during quiet and moderate wave conditions at the Sand Motor as a result of (tidal) flow contraction. This was shown from the strong correlation between the time-averaged mean bed shear stresses ( $\bar{\tau}_{cw,mean}$ ) and alongshore spatial heterogeneity of the  $D_{50}$  (Fig. 15), which indicates that a mechanism is present during moderate conditions (mainly due to the tide) which considerably affects the development of the spatial heterogeneity of the  $D_{50}$ . The added sediment at the Sand Motor was similar to that of the surrounding coast, while the potential

for mobilization was increased due to the tidal flow contraction at the peninsula. Consequently, the critical bed shear stresses for erosion of the fine fractions will be exceeded more frequently than for the coarser fractions, which results in a larger entrainment of the finer fractions in the water column (Komar, 1987) and enhanced alongshore transport rates (Steidtmann, 1982). For coasts with persistent erosion (i.e. larger outgoing than incoming flux of sediment), which is present at the large scale coastal disturbance of the Sand Motor, this will result in a coarsening of the bed in the coastal section with enhanced bed shear stresses and a fining of the bed at the adjacent coast where the flux of finer sand settles. The preferential transport of finer sand fractions will also be present when all fractions are mobilized, but it is expected to be strongest when the hydrodynamic forcing conditions are close to the critical bed shear stress of the considered sand fractions. On the basis of the observed gradual reduction of the  $S_{alongshore}$  (Fig. 13) it is expected that the coarser bed composition at the Sand Motor will have a tendency to fade out over time. This is attributed to reduced tidal forcing conditions over time as a result of the smoothing of the morphology of the Sand Motor.

### • II: Storm impact

Storm events can reduce the alongshore heterogeneity of the  $D_{50}$  at the Sand Motor, which is shown from the observed fining of the bed in the offshore zone during a severe storm condition (at 22 October 2014; T6 survey). This is in contrast with the coarsening of the bed (about 30  $\mu m$  coarser  $D_{50}$ ) that was observed by Terwindt (1962) during a storm event. The changes in  $D_{50}$  of the bed at the Sand Motor also differed from observations by Stauble and Cialone (1996), who observed only nearshore coarsening of the  $D_{50}$  (landward of MSL –3 m) and negligible changes in  $D_{50}$  at MSL –5 m. These studies were, however, performed for natural coasts which lack the strong curvature of the coast and associated continuous erosion that is present at the Sand Motor. The observed finer  $D_{50}$  of the bed

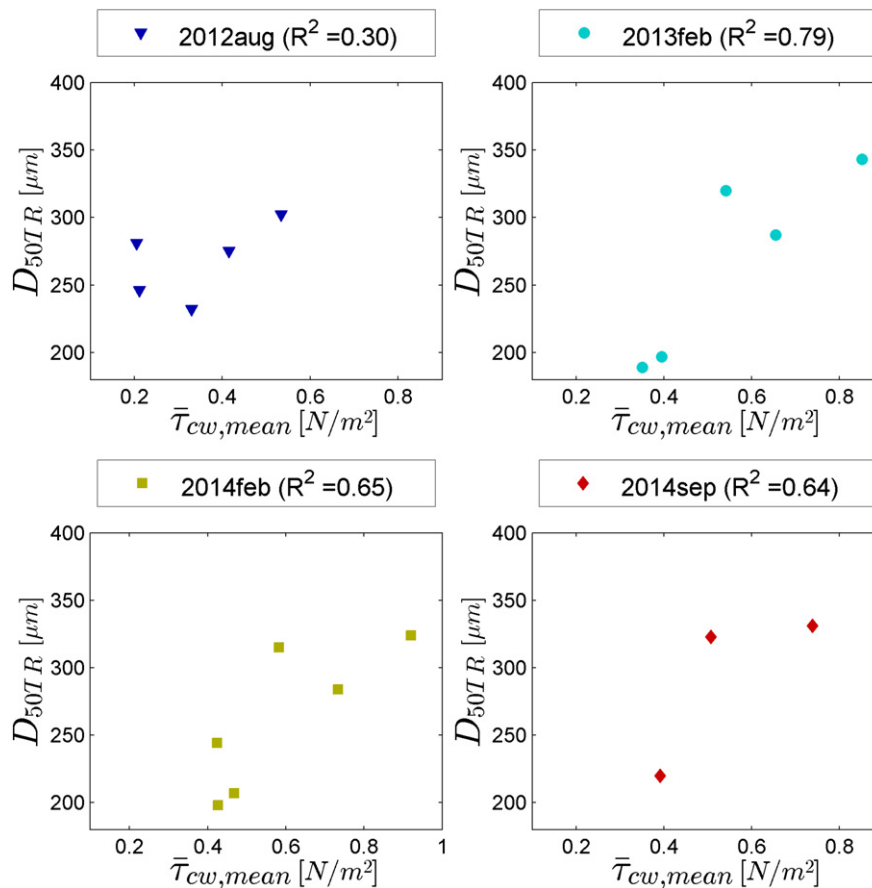


Fig. 16. Inter-relation between transect-averaged bed shear stress ( $\bar{\tau}_{cw,mean}$ ) and median grain diameter ( $D_{50TR}$ ) for T2, T3, T5 and T6 surveys.

in deeper water as a result of the 22 October 2014 storm is expected to be related to high-wave conditions which mobilize all sand grains. This means that also the coarser bed material will be mobilized and distributed. Part of the armor layer may be removed resulting in exposure of (and mixing with) substrate layers and consequently in a relatively finer top-layer of the bed. This is especially of relevance in deeper water where more time is available to develop an armored bed during normal conditions (i.e. before high-energetic events mobilize the bed and partially remove the armoring). Additionally, storm events transport finer sediment in the offshore direction which will result in a coarsening of the (erosive) nearshore zone and a fining in deeper water at the toe of the storm deposition profile, as was observed in the wave flumes at the Großer WellenKanal (Broekema et al., *in press*) and numerical modelling with Delft3D and Xbeach (Sirks, 2013; Reniers et al., 2013). Evidence of cross-shore transport of finer sand during storms was perceived to be present in the T2 survey for which a zone with relatively fine sand (i.e. 100 to 200  $\mu\text{m}$ ) was observed at 4 to 8 meter water depth.

- III: Initial bed composition

A part of the observed alongshore heterogeneity of the  $D_{50}$  at the Sand Motor can be attributed to the initial disturbance of the bed sediment during construction (e.g. coarser sand applied locally or as a result of suspension sorting). The sediment used for construction ( $278 \mu\text{m} \pm 60 \mu\text{m}$ ) was significantly coarser than the bed composition of the T0 survey ( $\sim 220 \mu\text{m}$ ). However, the gradual coarsening of the  $D_{50TR}$  at

the Sand Motor peninsula in the first two years after construction (from 278  $\mu\text{m}$  at T1 to 300 to 400  $\mu\text{m}$  at T4) indicates that the development of alongshore heterogeneity of the  $D_{50}$  was affected considerably by the hydrodynamic sorting processes. An exact estimate of the contribution of the initial bed composition changes during construction cannot be given on the basis of the data alone, since T1 samples were only taken at the dry beach. It may require extra data of the initial bed composition at future large-scale coastal measures and/or well validated numerical modelling to further improve understanding on the initial bed composition as a result of dredging and nourishing activities.

It is recognized that sediment sampling and methodology for determining the grain size distribution may affect the measured  $D_{50}$  at the Sand Motor. For example, the application of the Van Veen grabber inherently means that only the first five to ten centimeters of the bed sediment are sampled. Consequently, the underlying assumption in the interpretation is that a sufficiently thick layer of rather homogeneous sediment is present at the sample location. This does, however, seem like a realistic condition for a large-scale sand nourishment with persistent and steady patterns of erosion and sedimentation. The impact from the methodology for determining the grain size distribution was expected to be small for the current studies, since the current study focuses mainly on the median grain diameters ( $D_{50}$ ) which are shown to be better correlated for the different analysis techniques (Laser diffraction or sieving) than derived properties of the grain size distribution like Skewness and Kurtosis

(Murray and Holtum, 1996; Rodríguez and Uriarte, 2009). Moreover, the observed changes over time were more considerable than the uncertainty in the analysis methodology, as derived from a data set of mechanically sieved samples and corrected Laser diffraction samples.

The observed development of alongshore heterogeneity of the  $D_{50}$  at the Sand Motor is considered a relevant mechanism which may also act at other large scale coastal measures which induce an increase in the hydrodynamic forcing conditions (e.g. due to tidal contraction). The  $D_{50}$  of the bed is likely to coarsen as a result of the new situation with enhanced bed shear stresses, which is even the case when nourishment sand with similar properties as the natural sediment is applied. The alongshore heterogeneity of the  $D_{50}$  at large-scale coastal measures, such as the Sand Motor, is expected to have a considerable impact on long-term morphological changes and ecological habitats of marine fish and benthos. It is envisaged that the long-term morphological changes of the Sand Motor are slowed-down by the coarsening of the bed at the exposed coastal sections due to reduced sediment transport of the coarser sand. Initial morphological changes, on the other hand, may have been enhanced as a result of the initially large erosion rates of the fine sand fractions (i.e. compared to the situation with a very narrow grain size distribution). Ecological impact is expected from the coarsening of the bed at the Sand Motor peninsula and fining of the bed at the adjacent coast. The actual impact differs per species and may either be beneficial or adverse (Alexander et al., 1993; McLachlan, 1996). For example, the coarsening of the bed at the Sand Motor may limit the body size of marine species and burrowing ability of juvenile Plaice (Gibson and Robb, 1992), while an improvement of the habitat suitability may be expected at the adjacent coast where sediment is finer. Given above considerations, it is considered relevant to account for bed composition changes in the environmental impact assessments of future large-scale coastal measures.

## 7. Conclusions

Bed sediment composition ( $D_{50}$ ) was surveyed and analysed at the large-scale 'Sand Motor' nourishment at the Dutch coast (~21.5 million  $m^3$  sand) which is a large scale coastal perturbation which experiences continuous erosion. Significant spatial heterogeneity of the bed composition ( $D_{50}$ ) was observed, which consisted of a coarsening in front of the Sand Motor peninsula of +90 to +150  $\mu m$  and a fining of the sediment just north and south of the Sand Motor up to 50  $\mu m$  (referred to as 'alongshore heterogeneity of  $D_{50}$ '). Most pronounced alongshore heterogeneity of  $D_{50}$  was observed in deeper water outside the surfzone (seaward of MSL –4 m).

Spatial heterogeneity of the  $D_{50}$  can be induced by hydrodynamic forcing conditions at any large-scale coastal intervention which is sufficiently large to substantially affect the hydrodynamics of the tide. Alongshore spatial heterogeneity of the transect-averaged median grain size ( $D_{50TR}$  of coarsest and finest transect) was found to be strongly inter-related with the hydrodynamic forcing conditions as a result of the tide (i.e. time-averaged mean bed shear stresses). Preferential transport of finer sediment is a relevant mechanism for the coarsening of the bed at large scale coastal measures. The locally enhanced tidal forces mobilize in particular the finer sand fractions, while medium and coarse sand are hardly mobilized. The finer sediment is then transported to the adjacent coast. A requirement for this mechanism of preferential transport of finer sand fractions is a persistent pattern of erosion at the considered large-scale coastal measure, which means that the outgoing sediment flux exceeds the incoming flux of sand.

Storm conditions may reduce the coarsening of the bed in deeper water (i.e. outside the surfzone) for regions with enhanced bed shear stresses. This is the result of a mobilization of all of the bed sediment

size fractions during storms and exposure of relatively fine substrate material as a result of the erosion. Additionally, storms may generate a cross-shore flux of finer sand from the surfzone to deeper water.

## Acknowledgments

The European Research Council of the European Union is acknowledged for the funding provided for this research by the ERC-Advanced Grant 291206-NEMO. Also the Dutch Technology Foundation STW is acknowledged, as part of the Netherlands Organisation for Scientific Research (NWO), which is partly funded by the Ministry of Economic Affairs (project no. 12686; NatureCoast). Sampling data for the years 2010, 2012 and September 2013 were collected with support of the European Fund for Regional Development (EFRO) which was taken care of by Jeroen Wijsman of IMARES and Pieter-Koen Tonnon of Deltares. Special thanks go to my promotor Marcel Stive who has provided the excellent conditions for this research. Daan Wouwenaar, Saulo Meirelles, Emma Sirks, Jelle van der Zwaag and Laurens Bart are thanked for their support during the sediment surveys and processing of the samples.

## Appendix A. Computation of bed shear stresses

Bed composition changes ( $D_{50,TR}$ ) at the Sand Motor are related either to the forcing conditions of the (tidal) currents or (storm) waves. For this purpose, the mean and maximum bed shear stresses as a result of combined waves and currents ( $\tau_{cw,mean}$  and  $\tau_{cw,max}$ ) are used as a proxy for respectively the net hydrodynamic force of the local currents and the maximum forcing as a result of the wave orbital motion. The combined contribution of waves and currents ( $\tau_{cw,mean}$  [ $N/m^2$ ]) is computed as follows according to Soulsby et al. (1993):

$$\tau_{cw,mean} = Y(\tau_C + |\tau_W|) \quad (A1)$$

where  $\tau_C$  and  $\tau_W$  represent the current and wave related bed shear stress [ $N/m^2$ ]. The mean bed shear stress reduction factor ( $Y = X[1 + bX^p(1 - X)^q]$ ) is computed from the ratio of current and wave related bed shear stress ( $X = \tau_C/(\tau_C + \tau_W)$ ). Wave current-interaction coefficients  $b$ ,  $p$ ,  $q$  are set according to Van Rijn et al. (2004). The current related shear stress is computed on the basis of the average current velocity and friction with the bed.

$$\tau_C = \frac{1}{8} \rho_w f_c \bar{U} |\bar{U}| = \frac{\rho_w g \bar{U} |\bar{U}|}{C_{2D}} \quad (A2)$$

With  $\rho_w$  the density of the water [ $kg/m^3$ ],  $g$  the acceleration of gravity [ $m/s^2$ ],  $f_c$  the dimensionless friction factor of Darcy-Weisbach,  $\bar{U}$  the depth averaged current velocity [ $m/s$ ] and  $C_{2D}$  the Chezy coefficient [ $m^{1/2}/s$ ]. The wave related bed shear stress ( $\tau_W$ ) is computed as follows:

$$\tau_W = \frac{1}{4} \rho_w f_w (U_{\delta,r}^2) \quad (A3)$$

with  $U_{\delta,r}$  the orbital velocity of the waves [ $m/s$ ] according to Isobe and Horikawa (1982) and  $f_w$  the friction coefficient for waves [ $m$ ]. The friction factor for wave induced flow depends on the peak orbital excursion of the waves at the edge of the wave boundary layer ( $A_b$ )



and the bed form induced roughness ( $k_{s,w,r}$ ) which is related to the flow regime (e.g. sheet-flow or ripple regime; Van Rijn et al., 2004).

$$f_w = \exp\left(5.2\left(\frac{A_\delta}{k_{s,w,r}}\right)^{-0.19} - 6\right) \quad (\text{A4})$$

Similar to the mean bed shear stress ( $\tau_{cw,mean}$ ) also the maximum bed shear stress ( $\tau_{cw,max}$ ) is computed:

$$\tau_{cw,max} = Z(\tau_c + |\tau_w|) \quad (\text{A5})$$

With maximum bed shear stress reduction factor ( $Z = 1 + aX^m(1 - X)^n$ ) and  $a$ ,  $m$  and  $n$  as the wave current interaction coefficients (Soulsby et al., 1993).

## Appendix B. Width and skewness of the distribution

Graphical sample standard deviation ( $\sigma_I$ ) and graphical skewness ( $Sk_I$ ) of the grain size distribution (Folk and Ward, 1957) were computed as follows from the  $\phi$  values of the sediment (i.e.  $\phi = -\log_2(D)$ , with  $D$  as the grain diameter in millimeters).

$$\sigma_I = \frac{\phi_{84} - \phi_{16}}{4} + \frac{\phi_{95} - \phi_5}{6.6} \quad (\text{B1})$$

$$Sk_I = \frac{\phi_{16} + \phi_{84} - 2 * \phi_{50}}{2(\phi_{84} - \phi_{16})} + \frac{\phi_5 + \phi_{95} - 2 * \phi_{50}}{2(\phi_{95} - \phi_5)} \quad (\text{B2})$$

These derived properties can provide insight in the processes that were driving the bed composition changes. An overview of the observed graphical standard deviation ( $\sigma_I$ ) and skewness ( $Sk_I$ ) of the grain size distribution are provided in Figs. B1 and B2.

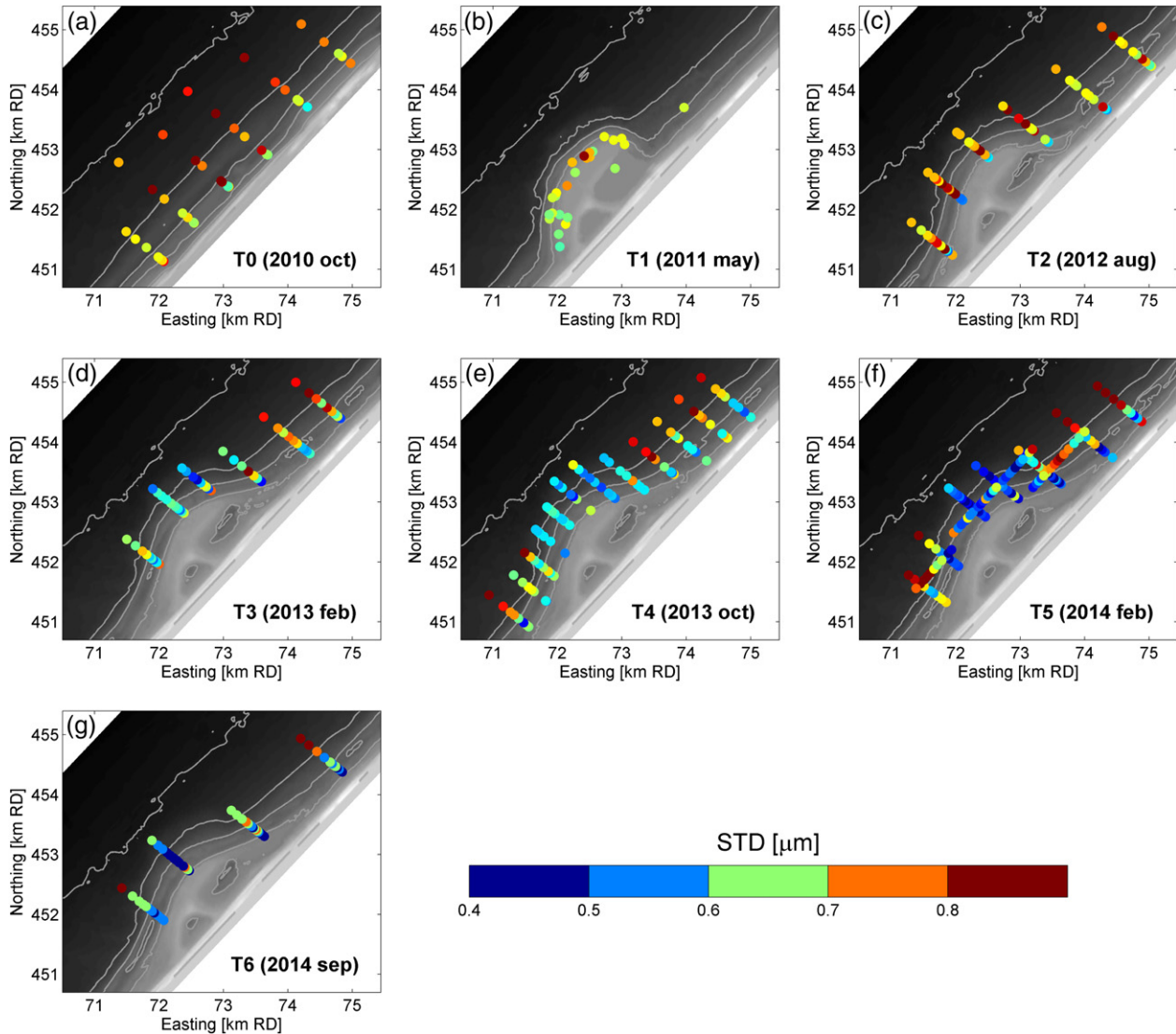
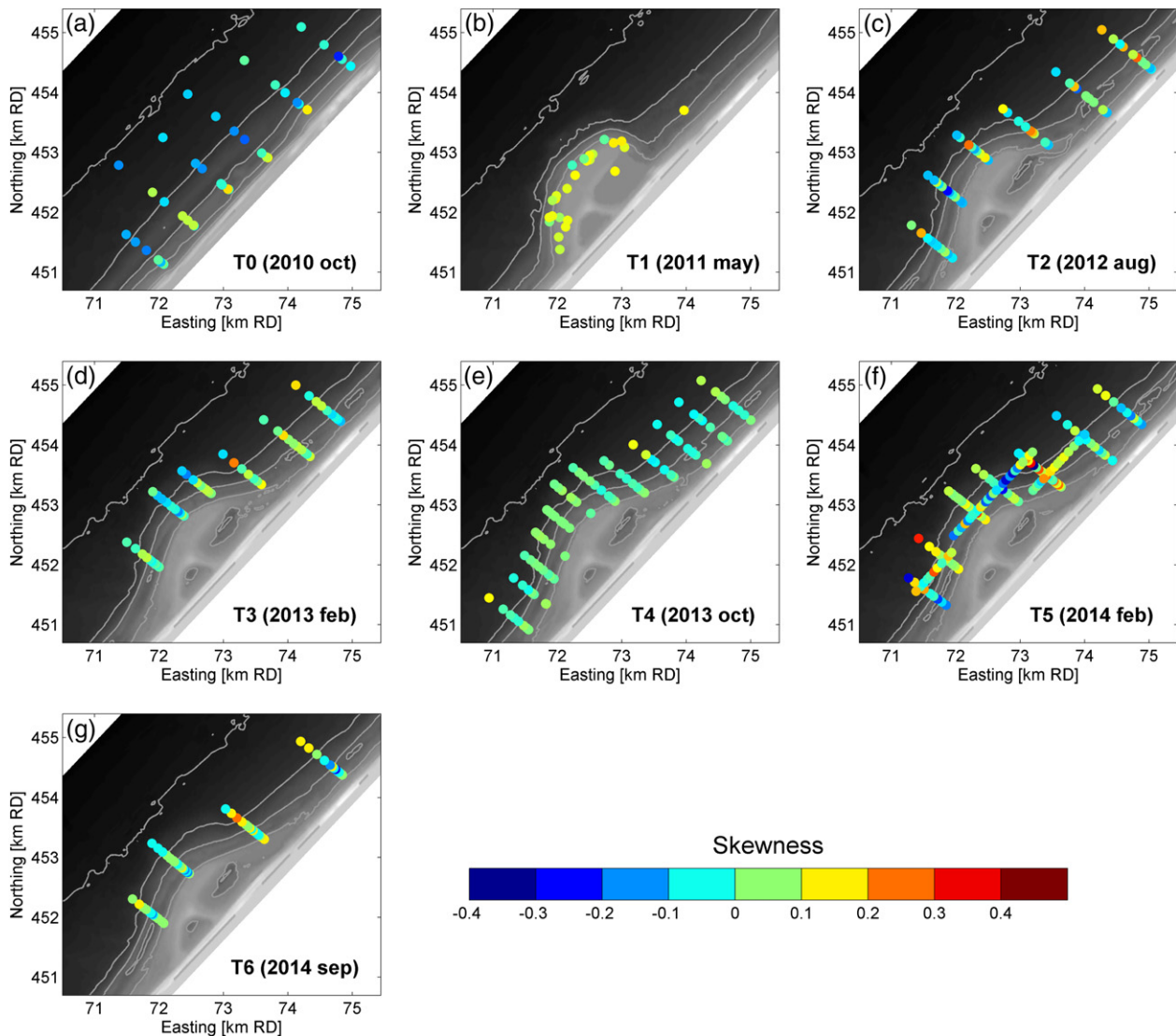


Fig. B1. Standard deviation of sediment samples for T0 to T6 measurement surveys (blue colours indicate better sorted sand and red colours more poorly sorted sand).



**Fig. B2.** Graphical skewness of sediment samples for T0 to T6 measurement surveys (red indicates fine skewed sand; blue indicates coarse skewed sand).

The reference survey samples (T0) and original nourished material (T1) were moderately sorted to moderately well sorted (i.e.  $\sigma_I$  ranging from 0.6 to 0.8). This is in contrast with the situation from survey T3 onwards, which shows considerable spatial variability in the width of the grain size distribution ( $\sigma_I$ ). This spatial variability comprised a relatively narrow grain size distribution (i.e.  $\sigma_I$  of 0.4 to 0.6) at the center transect of the Sand Motor and more poorly sorted sand (i.e.  $\sigma_I$  of 0.7 to 0.9) in deeper water (from MSL –5 m to MSL –10 m) at the adjacent coast North and South of the Sand Motor. Noticeable is that the 10th weight percentile of the grain size ( $D_{10}$ ) at the center transect of the Sand Motor (transect D) has coarsened significantly after construction of the Sand Motor (from 124  $\mu$ m in the reference situation to ~220  $\mu$ m from T3 survey onwards at transect D and E), which is an indication for sorting of the sediment by the transport processes (McLaren and Bowles, 1985; Masselink, 1992).

Graphical skewness ranged from fine skewed to coarse skewed ( $Sk_I$  of –0.2 to +0.2) for the T0 survey (Fig. B2) and was generally

smaller in deeper water than near to the shoreline. Samples with an excess of fines were found landward of MSL –3 m for the T0 survey. After construction of the Sand Motor some of the deep water sample locations of the T3 to T5 surveys were fine skewed to very fine skewed, which was typically the case for depositional areas where fine sand and silt from the Sand Motor accumulated.

Short-term temporal variability of the graphical standard deviation of the grain size distribution ( $\sigma_I$ ) was small during the T6 survey (Fig. B3). The  $\sigma_I$  of the bed at the sub-tidal bar was ~0.4 and increased in landward direction to ~0.8 in the bar trough and in seaward direction to ~0.6 at MSL –10 m. Similarly, the temporal variability of the observed graphical skewness ( $Sk_I$ ) was also small. Only after the storm condition a more coarse skewed grain size distribution was observed in the bar trough ( $Sk_I \sim -0.2$ ) and a fine skewed distribution ( $Sk_I \sim +0.2$ ) at MSL –6 m to MSL –8 m.

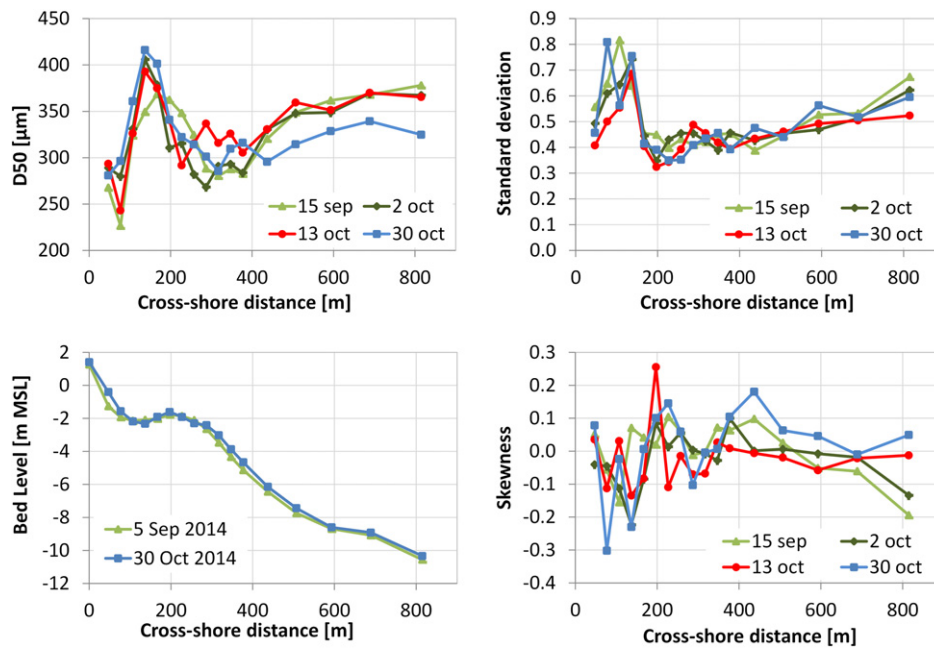


**Fig. B3.** Median grain diameter ( $D_{50}$ ), graphical standard deviation ( $\sigma_1$ ), graphical skewness ( $Sk_1$ ) and bed level for T6 measurement survey at transect D (i.e. center of Sand Motor).

### Appendix C. Transect-averaged median grain diameter

The transect-averaged median grain diameters ( $D_{50TR}$ ) were computed for each of the transects from the waterline up to MSL –10 m (Table C.1). Additionally, also the median grain diameters were computed for the surfzone landward of MSL –4 m ( $D_{50TR,NS}$ ) and the less active offshore part of the cross-shore profile ( $D_{50TR,OFF}$ ). Note that an average of nearby transects was used for some of the transects of surveys T0, T2 and T4 that did not exactly align with the transect positions of the T5 survey transects (A to G).

**Table C.1**

Average median grain diameter per transect ( $D_{50TR}$ ) and differentiated for the zone seaward and landward of the MSL –4 m ( $D_{50TR,OFF}$  and  $D_{50TR,NS}$ ) of the T0 to T6 surveys at the Sand Motor.

Transect	T0 oct 2010			T2 aug 2012			T3 feb 2013			T4 oct 2013			T5 feb 2014			T6 oct 2014		
	$D_{50TR}$			$D_{50TR}$			$D_{50TR}$			$D_{50TR}$			$D_{50TR}$			$D_{50TR}$		
	avg	OFF	NS	avg	OFF	NS	avg	OFF	NS	avg	OFF	NS	avg	OFF	NS	avg	OFF	NS
A	227	226	241	353	354	349	251	254	232	273	288	232	241	229	304	262	268	242
F	208	207	224	281	289	269	197	183	255	221	201	306	198	188	246			
B	231	210	285	245	233	264	189	162	288	220	201	282	207	175	284	220	183	309
C							287	276	330	280	289	261	284	218	289	268	248	257
D	216	200	304	302	305	296	343	347	333	354	359	345	324	327	319	331	338	320
E	226	220	263	267	293	205	320	320	320	321	318	327	315	323	302	323	328	315
G	214	204	239	246	243	253				248	205	347	244	195	340			
AVG*	220	211	260	282	286	273	264	257	293	275	266	304	259	245	298	281	273	292

\*Weighted average of all transects



## References

- Alexander, R.R., Stanton, R.J., Dodd, J.R., 1993. Influence of sediment grain size on the burrowing of bivalves. *Palaios* 8, 289–303.
- Baba, J., Komar, P.D., 1981. Measurements and analysis of settling velocities of natural quartz sand grains. *J. Sediment. Petrol.* 51, 631–640.
- Booij, N., Ris, R.C., Holthuijsen, L.H., 1999. A third-generation wave model for coastal regions 1. Model description and validation. *J. Geophys. Res.* 104 (C4), 7649–7666. (C4).
- Broekema, Y.B., Giardino, A., Van der Werf, J.J., Van Rooijen, A.A., Voudoukas, M.I., Van Prooijen, B.C., 2016. Observations and modelling of nearshore sediment sorting processes along a barred beach profile. *Coast. Eng.* ISSN 0378-3839. <http://dx.doi.org/10.1016/j.coastaleng.2016.08.009>. (in press).
- BS812, 1975. Sampling, Shape, Size and Classification, Part I. 1975, British Standards (BS), 812. British Standard Institution, London.
- Capobianco, M., Hanson, H., Larson, M., Steetzel, H., Stive, M.J.F., Chatelus, Y., Aarninkhof, S., Karambas, T., 2002. Nourishment design and evaluation: applicability of model concepts. *Coast. Eng.* 47 (2), 113–135.
- de Schipper, M.A., de Vries, S., Ruessink, G., de Zeeuw, R.C., Rutten, J., van Gelder-Maas, C., Stive, M.J., 2016. Initial spreading of a mega feeder nourishment: observations of the sand engine pilot project. *Coast. Eng.* 111, 23–38.
- Dong, P., Chen, Y., Chen, S., 2015. Sediment size effects on rip channel dynamics. *Coast. Eng.* 99, 124–135.
- Eisma, D., 1968. Composition, origin and distribution of Dutch coastal sands between Hoek van Holland and the Island of Vlieland. *Neth. J. Sea Res.* 4, 123–267.
- Folk, R.L., Ward, W.C., 1957. Brazos River bar: a study in the significance of grain size parameters. *J. Sediment. Petrol.* 27, 3–26.
- Gallagher, E.L., MacMahan, J.H., Reniers, A.J.H.M., Brown, J.A., Thornton, E.B., 2011. Grain size variability on a rip-channel beach. *Mar. Geol.* 287, 43–53.
- Gao, S., Collins, M., 1992. Net sediment transport patterns inferred from grain-size trends based upon definitions of “transport vectors”. *Sediment. Geol.* 80, 47–60.
- Gibson, R.N., Robb, L., 1992. The relationship between body size, sediment grain size and the burying ability of juvenile plaice, *Pleuronectes platessa* L. *J. Fish Biol.* 40, 771–778.
- Guillén, J., Hoekstra, P., 1996. The “equilibrium” distribution of grain size fractions and its implications for cross-shore sediment transport: a conceptual model. *Mar. Geol.* 135, 15–33.
- Guillén, J., Hoekstra, P., 1997. Sediment distribution in the nearshore zone: grain size evolution in response to shoreface nourishment (Island of Terschelling, The Netherlands). *Estuar. Coast. Shelf Sci.* 45, 639–652.
- Holland, K.N., Elmore, P.A., 2008. A review of heterogeneous sediments in coastal environments. *Earth Sci. Rev.* 89, 116–134.
- Horn, D.P., 1993. Sediment dynamics on a macrotidal beach, Isle of Man (U.K.). *J. Coast. Res.* 9, 189–208.
- Inman, D.L., 1953. Areal and seasonal variations in beach and nearshore sediments at La Jolla, California. *Tech. rep. 39. U.S. Army Corps Eng. Beach Erosion Board, Technical Memorandum.*
- Isobe, M., Horikawa, K., 1982. Study on water particle velocities of shoaling and breaking waves. *Coast. Eng. Jpn* 25, 109–123.
- Janssen, G.M., Mulder, S., 2005. Zonation of macrofauna across sandy beaches and surf zone along the Dutch coast. *Oceanologia* 47, 265–282.
- Kana, T.W., Rosati, J.D., Traynum, S.B., 2011. Lack of evidence for onshore sediment transport from deep water at decadal time scales: Fire Island, New York. *J. Coast. Res.* 51 59, 61–75.
- Katoh, K., Yanagishima, S., 1995. Changes of sand grain distribution in the surf zone. In: Zeidler, R.B., Dally, W.R. (Eds.), *Coastal Dynamics 95: Proceedings of the International Conference on Coastal Research. Am. Soc. of Civ. Eng., Gdansk, Poland*, pp. 639–650.
- Knaapen, M.A.F., Holzhauser, H., Hulscher, S.J.M.H., Baptist, M.J., De Vries, M.B., Van Ledden, M., 2003. On the modelling of biological effects on morphology. *River, Coastal and Estuarine Morphodynamics Barcelona*. pp. 773–783.
- Komar, P.D., 1987. Selective grain entrainment by a current from a bed of mixed sizes: a reanalysis. *J. Sediment. Petrol.* 57 (2), 203–211.
- Konert, M., Vandenberghe, J., 1997. Comparison of laser grain size analysis with pipette and sieve analysis: a solution for the underestimation of the clay fraction. *Sedimentology* 44, 523–535.
- Lesser, G.R., Roelvink, J.A., van Kester, J.A.T.M., Stelling, G.S., 2004. Development and validation of a three-dimensional morphological model. *Coast. Eng.* 51 (8–9), 883–915.
- Liu, J.T., Zarillo, G.A., 1987. Partitioning of shoreface sediment grain-sizes. *Coastal Sediments, New Orleans, USA*. pp. 1533–1548.
- Luijendijk, A.P., Huisman, B.J.A., De Schipper, M.A., Walstra, D.J.R., Ranasinghe, R., 2016. On the relevance of forcing conditions for the initial response of the sand engine pilot project. *Coast. Eng.* (in press).
- MacMahan, J., Stanton, T.P., Thornton, E.B., Reniers, A.J.H.M., 2005. RIPEX-Rip Currents on a shore-connected shoal beach. *Mar. Geol.* 218, 113–134.
- Masselink, G., 1992. Longshore variation of grain-size distribution along the coast of the Rhone Delta, Southern France – a test of the McLaren model. *J. Coast. Res.* 8 (2), 286–291.
- McLachlan, A., 1996. Physical factors in benthic ecology: effects of changing sand particle size on beach fauna. *Mar. Ecol. Prog. Ser.* 131, 205–217.
- McLaren, P.A., Bowles, D., 1985. The effects of sediment transport on grain-size distributions. *J. Sediment. Petrol.* 55, 457–470.
- Medina, R., Losada, M.A., Losada, I.J., Vidal, C., 1994. Temporal and spatial relationship between sediment grain size and beach profile. *Mar. Geol.* 118, 195–206. 3.
- Moutzouris, C.I., Kraus, N.C., Gingerich, K.J., Kriebel, D.L., 1991. Beach profiles versus cross-shore distributions of sediment grain sizes. *Adv. Coast. Model.* 860–874. (American Society of Civil Engineers, New York, NY).
- Murray, D.M., Holtum, D.A., 1996. Technical note: inter-conversion of malvern and sieve size distributions. *Miner. Eng.* 9 (12), 1263–1268.
- Pruszek, Z., 1993. The analysis of beach profile changes using dean's method and empirical orthogonal functions. *Coast. Eng.* 19, 245–261.
- Radermacher, M., Zeelenberg, W., De Schipper, M.A., Reniers, A.J.H.M., 2015. Field observations of tidal flow separation at a mega-scale beach nourishment. *The Proceedings of the Coastal Sediments 2015. San Diego, USA*, 11–15 May 2015.
- Reniers, A.J.H.M., Gallagher, E.L., MacMahan, J.H., Brown, J.A., van Rooijen, A.A., van Thiel de Vries, J.S.M., van Prooijen, B.C., 2013. Observations and modeling of steep-beach grain-size variability. *J. Geophys. Res. Oceans* 118 (2), 577–591.
- Richmond, B.M., Sallenger, A.H.J., 1984. Cross-shore transport of bimodal sands. *Proceedings of the 19th International Conference on Coastal Engineering*. 2. pp. 1997–2008.
- Rodriguez, J.G., Uriarte, A., 2009. Laser diffraction and dry-sieving grain size analyses undertaken on fine- and medium-grained sandy marine sediments: a note. *J. Coast. Res.* 25 (1), 257–264.
- Rubin, D.M., 2004. A simple autocorrelation algorithm for determining grain size from digital images of sediment. *J. Sediment. Res.* 74 (1), 160–165.
- Sembiring, L.E., van Ormondt, M., van Dongeren, A.R., Roelvink, J.A., 2015. A validation of an operational wave and surge prediction system for the Dutch Coast. *Nat. Hazards Earth Syst. Sci. Discuss.* 2, 3251–3288.
- Sirks, E.E., 2013. Sediment Sorting at a Large Scale Nourishment. Delft University of Technology. (Master's thesis)
- Slingerland, R., Smith, N.D., 1986. Occurrence and formation of water-laid placers. *Annu. Rev. Earth Planet. Sci.* 14, 113–147.
- Sonu, C., 1972. Bimodal composition and cyclic characteristics of beach sediment in continuously changing profiles. *J. Sediment. Petrol.* 42, 852–857.
- Soulsby, R.L., Hamm, L., Klopman, G., Myrhaug, D., Simons, R.R., Thomas, G.P., 1993. Wave-current interaction within and outside the bottom boundary layer. *Coast. Eng.* 21, 4169.
- Stauble, D.K., Cialone, M.A., 1996. Sediment dynamics and profile interactions: Duck94. *Coast. Eng.* 4, 3921–3934.
- Steidtmann, J.R., 1982. Size-density sorting of sand-size spheres during deposition from bedload transport and implications concerning hydraulic equivalence. *Sedimentology* 29, 877–883.
- Stive, M.J.F., De Schipper, M.A., Luijendijk, A.P., Aarninkhof, S.G.J., Van Gelder-Maas, C., Thiel de Vries, J. S. M., Van, De Vries, S., Henriquez, M., Marx, S., Ranasinghe, R., 2013. A new alternative to saving our beaches from sea-level rise: the sand engine. *J. Coast. Res.* 29 (5), 1001–1008.
- Terwindt, J.H.J., 1962. Study of grain size variations at the coast of Katwijk 1962 (in Dutch). Report K-324. Rijkswaterstaat, The Hague, The Netherlands.
- Van Rijn, L.C., 1993. Principles of Sediment Transport in Rivers, Estuaries and Coastal Seas. Aqua Publications, Amsterdam.
- Van Rijn, L.C., 2007. Unified view of sediment transport by currents and waves III: graded beds. *J. Hydraul. Eng.* 133 (7), 761–775.
- Van Rijn, L.C., Walstra, D.J.R., van Ormondt, M., 2004. Description of TRANSPOR2004 and impelmentation in Delft3D-ONLINE. Report Z3748.00. WL | Delft Hydraulics.,
- Van Straaten, L.M.J.U., 1965. Coastal barrier deposits in South- and North Holland in particular in the area around Scheveningen and IJmuiden. *Mededelingen van de Geologische Stichting* 17, 41–75.
- Weber, O., Gonthier, E., Faugères, J.C., 1991. Analyse granulométrique de sédiments fins marins: comparaison des résultats obtenus au sédiograph et au malvern. *Bull. Institut Géol. Bassin Aquitaine* 50, 107–114.
- Wijnberg, K.M., 2002. Environmental controls on decadal morphologic behaviour of the Holland coast. *Mar. Geol.* 189, 227–247.
- Wijnberg, K.M., Kroon, A., 2002. Barred beaches. *Geomorphology* 48, 103–120.
- Wijsman, J.W.M., Verduin, E., 2011. TO monitoring Zandmotor Delftlandse kust: Benthos ondiepe kustzone en natte strand. *Tech. rep. IMARES / Wageningen UR*.
- Zonneveld, P.C., 1994. Comparative investigation of grain-size determination (sieve/Malvern). State Geological Survey, Haarlem, The Netherlands.